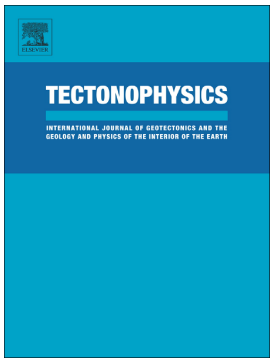

Cenozoic intraplate tectonics in Central Patagonia: Record of main Andean phases in a weak upper plate

G.M. Gianni, A. Echaurren, A. Folguera, J. Likerman, A. Encinas, H.P.A. García, C. Dal Molin, V.A. Valencia

PII: S0040-1951(17)30406-7
DOI: doi:10.1016/j.tecto.2017.10.005
Reference: TECTO 127643

To appear in: *Tectonophysics*

Received date: 12 May 2017
Revised date: 24 August 2017
Accepted date: 1 October 2017

Please cite this article as: G.M. Gianni, A. Echaurren, A. Folguera, J. Likerman, A. Encinas, H.P.A. García, C. Dal Molin, V.A. Valencia , Cenozoic intraplate tectonics in Central Patagonia: Record of main Andean phases in a weak upper plate. The address for the corresponding author was captured as affiliation for all authors. Please check if appropriate. Tecto(2017), doi:10.1016/j.tecto.2017.10.005

Cenozoic intraplate tectonics in Central Patagonia: Record of main Andean phases in a weak upper plate

G. M. Gianni[1], A. Echaurren[2], A. Folguera[2], J. Likerman[2], A. Encinas[3], H.P.A. García[1], C. Dal Molin[4], V. A.Valencia[5]

[1]IGSV. Instituto Geofísico Sismológico Ing. F. Volponi. Universidad Nacional de San Juan. CONICET. Km 12, jardín de los Poetas, Rivadavia (5400), San juan, Argentina.

[2] IDEAN, Instituto de Estudios Andinos Don Pablo Groeber, UBA - CONICET. Departamento de Ciencias Geológicas, FCEN, Universidad de Buenos Aires.

[3] Departamento de Ciencias de la Tierra, Universidad de Concepción, Casilla 160-C, Concepción, Chile.

[4]SEGEMAR, Av. Julio Argentino Roca 651, Buenos Aires, Argentina. CP (C1067ABB).

[5]School of the Environment, Washington State University, Pullman, Washington 99164, USA

Corresponding author: Guido M. Gianni (guidogianni22@gmail.com)

Abstract

Contraction in intraplate areas is still poorly understood relative to similar deformation at plate margins. In order to contribute to its comprehension, we study the Patagonian broken foreland (PBF) in South America whose evolution remains controversial. Time constraints of tectonic events and structural characterization of this belt are limited. Also, major causes of strain location in this orogen far from the plate margin are enigmatic. To unravel tectonic events, we studied the Cenozoic sedimentary record of the central sector of the Patagonian broken foreland (San Bernardo fold and thrust belt, 44º30'S-46ºS) and the Andes (Meseta de Chalia,46ºS) following an approach involving growth-strata detection, U-Pb geochronology and structural modeling. Additionally, we elaborate a high resolution analysis of the effective elastic thickness (Te) to examine the relation between intraplate contraction location and zones of low lithospheric strength. The occurrence of Eocene growth-strata (~44-40 Ma) suggests that

contraction in the Andes and the Patagonian broken foreland was linked to the Incaic phase. Detection of synextensional deposits suggests that the broken foreland collapsed partially during Oligocene to early Miocene. During middle Miocene times, the Quechua contractional phase produced folding of Neogene volcanic rocks and olistostrome deposition at ~17 Ma. Finally, the presented Te map shows that intraplate contraction related to Andean phases localized preferentially along weak lithospheric zones (Te<15 km). Hence, the observed strain distribution in the PBF appears to be controlled by lateral variations in the lithospheric strength. Variations in this parameter could be related to thermo-mechanical weakening produced by intraplate rifting in Paleozoic-Mesozoic times.

Keywords: Intraplate contraction, Andean phases, broken foreland, growth-strata, elastic thickness

1. Introduction

The presence of intraplate contractional zones remote from plate boundaries, as uplifted basement blocks and inverted rift basins, has captured the attention of geoscientists worldwide (Duff and Langworthy, 1974; Hamilton, 1988; Ziegler et al., 1998, among others). Intraplate tectonic activity is mostly produced by far-field stresses linked to contemporaneous convergence in active margins (Ziegler et al., 1998). Most prominent examples are found up to ~1600 km from plate boundaries in close relation to collisional orogenic events (e.g. Cunningham, 2005; Yang and Liu, 2009). However, there are numerous regions of more subtle intraplate deformation linked to non-collisional or Cordilleran orogenic activity, that represent nevertheless significant tectonic events (e.g. Dickinson and Snyder, 1978; Ramos et al., 2002). Intraplate contraction is comparatively rare in the geological record, and consequently is poorly understood relative to contractional belts formed at plate margins (Raimondo et al., 2014). To become comparable with our knowledge of active margin orogens, a significant improvement in structural characterization, kinematics and time constraints of intraplate tectonic events, is needed (Aitken et al., 2013). In this connection, the study of modern examples is of paramount importance to shed light on this issue. Notably, much of the knowledge about this process arises from ancient examples where the absence of a preserved plate kinematic framework hampers a linkage of intraplate and plate margin processes (Xu et al., 2016). In this study, we focus on the central sector of the Patagonian broken foreland (PBF) (44º-46ºS) (Bilmes et al., 2013), a barely

addressed intraplate contractional zone in Central Patagonia (Figs. 1a and b), to better understand intraplate deformation related to Andean-type margins. This belt occupies a broad area of deformation characterized by a general NNW-trend and a latitudinal extent of ~750 km (Fig. 1b). Recent studies unraveled its earliest contractional stages in the Early Cretaceous (e.g., Giacosa et al., 2010; Gianni et al., 2015a; Navarrete et al., 2015; Echaurren et al., 2016), but much remains to be learnt about the Cenozoic evolution of the PBF. For instance, while a contractional stage has been acknowledged in late Cenozoic times (Homovc et al., 1995; Peroni et al., 1995; Giacosa et al., 2010; Bilmes et al., 2013), contrasting tectonic regimes have been proposed for the early Cenozoic stage ((contractional, Gianni et al., (2015a); Paredes et al.,(2006) vs extensional, Foix et al., (2013)). Also, along strike geochronological constraints on the most recent Neogene deformational event are limited to the Gastre Basin in the northern sector of the PBF (Bilmes et al., 2013), while similar data are lacking in the rest of this intraplate zone (Fig. 1b). More importantly, the reason why contraction localized in the Patagonian interior far from the plate margin is still enigmatic. It has been previously speculated that a weak lithosphere in Central Patagonia was critical for intraplate deformation (e.g. Bilmes et al., 2013; Gianni et al., 2015a; Echaurren et al., 2016). However, a clear spatial correlation between location of contractional structures and zones of weakened lithosphere has not been demonstrated yet. Hence, in this study we aim to recognize tectonic stages in Cenozoic times and then to discuss major controls on intraplate deformation location in the PBF. To unravel Cenozoic deformational stages, we examine the sedimentary record of the San Bernardo fold and thrust belt (FTB) and the North Patagonian Andes in the Meseta de Chalia (Fig. 1c), reconstructing their evolution through field mapping, structural analysis and U-Pb geochronology of syntectonic strata. Additionally, we integrate new field data with previously published data in a balanced structural cross section to comprehend the regional structure and quantify shortening. Finally, to understand the relationship between lithospheric strength and intraplate contraction in the PBF, we carried out an analysis of effective elastic thickness (Te), as a proxy for long-term lithospheric strength, following the results of Watts (1995) and Mouthereau et al. (2013). These authors showed that deformation localization and structural style in different orogens around the world largely correlate with the Te. Thus, a high-resolution map of spatial variations of Te in Central Patagonia was constructed from the relation between gravimetric anomalies and the topographic loads using spectral methods (e.g. Watts, 2001).

2. Geological background of the Patagonian foreland zone

The pre-Andean evolution of Central Patagonia in Mesozoic times was linked to the development of several intraplate rifts produced by the break-up of Western Gondwana. During the Early Jurassic a regional extensional event developed a NNW-trending retroarc marine/continental basin in Central Patagonia (e.g. Suárez and Márquez, 2007). Heralding continental break-up, Middle Jurassic times were characterized by rapid rift propagation onboard the Patagonian region (Uliana et al., 1989), where several extensional depocenters developed associated with the eruption of voluminous successions of silicic volcanic rocks (Pankhurst et al., 1998). Subsequently, during the latest stages of Western Gondwana break-up in Late Jurassic to Early Cretaceous times, renewed extension gave place to the development of the Río Mayo Sub-basin at the western margin of Central Patagonia (Aguirre Urreta and Ramos, 1981; Suárez et al., 2009) (Fig. 1c). To the east, opening of the San Jorge Gulf Basin took place in an intraplate setting (Figari et al., 1999) (Fig. 1c). Extension in Patagonia came to an end when the first oceanic floor consolidated in the South Atlantic Ocean (~130 Ma) (Fitzgerald et al., 1990). Then, the North Patagonian Andes began their uplift soon after ocean opening in Aptian times (Aguirre Urreta and Ramos, 1981; Folguera and Iannizzotto, 2004; Suárez et al., 2009; Echaurren et al., 2017). This switch in the tectonic regime is also well recorded to the north of the study area in the Southern Central Andes (e.g. Fennell et al., 2015; García-Morabito et al., 2012) and to the south in the Austral and Fueguian Andes (e.g. Klepeis et al., 2010; Ghiglione et al., 2014). From late Early to Late Cretaceous, initial intraplate contraction took place in the PBF as indicated by surface/subsurface evidences of synorogenic growth-strata in continental beds of the Chubut Group (Allard et al., 2015; Gianni et al., 2015a,2015b; Navarrete et al., 2015) , as well as, thermochronological analyses (Savignano et al., 2016) (Fig. 2). During Cenozoic times, which are the focus of this study, a Danian Atlantic-derived transgression flooded the foreland area (Figs. 1c and 2). In late Paleocene, deposition of the Río Chico Group took place in the surroundings of the San Bernardo FTB and the Deseado Massif to the south (Figs. 1c and 2). Noteworthy, the tectonic setting of these deposits is still debated, while scarce seismic data suggest synorogenic deposition to the west and south of the San Bernardo FTB (Gianni et al., 2015a; Navarrete et al., 2015), field information in the eastern San Jorge Gulf Basin points out to deposition during extension (Foix et al., 2013).

Sedimentation at this time was continental with fluctuations between fluvial and lacustrine conditions (Raigemborn et al., 2010; Krause et al., 2017). From base to top the Rio Chico Group is made up of four units: Las Violetas, Peñas Coloradas, Las Flores and Koluel-Kaike Formations. During the Eocene to early Miocene, deposition of pyroclastic materials reworked by fluvial systems (Sarmiento Group), coexisted with eruption of mafic rocks with a within-plate geochemical signature (Bruni et al., 2008) (Figs. 1 and 2). At the end of this stage in the early-middle Miocene, a second Atlantic-derived transgression flooded the Patagonian region (see Barreda and Bellosi, 2014) (Fig. 1). Particularly, the uppermost marine deposits corresponding to this event are known in the study area as "Suprapatagoniense beds" (Figs. 1 and 2). Subsequently, this transgressive marine sequence was replaced by different estuarine to fluvial units that evolved up to late Miocene times in a context of renewed Andean orogenesis to the west (Flint et al., 1994; Lagabrielle et al., 2004; Blisniuk et al., 2005) and intraplate contraction to the east in the PBF (Homovc et al., 1995; Peroni et al., 1995). Middle Miocene to Pliocene synorogenic deposits related to the last Andean uplift phase at studied latitudes are preserved in the Meseta the Chalia west of the San Bernardo FTB (Dal Molin and Franchi, 1996) (Fig. 1c).

3. Description of syntectonic sedimentation in the San Bernardo FTB and the Meseta de Chalía

Growth-strata detection is helpful to determine deformational events as syntectonic deposition tracks the evolution of individual structures (Riba, 1976). In order to detect growth structures in the study area we followed a classic approach similar to Arriagada et al. (2006) and Horton et al. (2015) based on direct measurements of strata dip and thickness changes. To avoid mistaking syntectonic deposits with strata divergence and thickening caused by trishear folding, we only studied those regions devoid of pervasive shearing. Additionally, we identified diverse features commonly present on syntectonic deposits (e.g. sedimentary onlaps and angular unconformities).

The San Bernardo FTB presents a western sector where Cretaceous strata and Miocene volcanic rocks crop out related to thick- and minor thin-skinned deformation and a less deformed eastern sector that preserves a complete Cenozoic sedimentary record (Fig. 2). In different localities of this last sector, we identified evidences of syntectonic deposition in the Eocene continental deposits of the upper Río Chico Group (Koluel Kaike Formation).

To the south of the Colhué Huapi Lake (Fig. 2) a series of west-vergent growth-folds are found in fluvial tuffaceous sandstones and siltstones of the Koluel Kaike Formation (Fig. 3). These, are characterized by fanning strata related to bed thickening and progressive dip variations (Fig. 3a,b,c). Particularly, the presence of a thrust-growth in that area related to a detaching sheet in the Koluel Kaike Formation indicates that syntectonic deposits were linked to a contractional regime (Fig. 3d). South of the study area, the Koluel Kaike Formation is present at both gently dipping flanks of a westward verging anticline (Fig. 4). This structure is part of a series of NNE-trending folds associated with the Grande-Funes anticline, related to a thrust detached in Neocomian levels (Fitzgerald et al., 1990). At the backlimb of this structure, syn-tectonic deposition of the Koluel Kaike Formation is evidenced by growth onlap relations and an internal angular unconformity (Fig. 4).

West of the PBF, over the Andean foothills, Eocene syntectonic sedimentation is also recorded in the Meseta de Chalía (Fig. 1). Here, a succession of continental sedimentary rocks divided into several formations by Dal Molin and Franchi (1996) (Pedregoso Formation, Miocene; Río Mayo Formation, Mio-Pliocene and Chalía Formation, Pliocene) are deformed by west-vergent folds interpreted as related to a backthrust system, adjacent to a gently dipping (10-5°E) sector to the east (Figs. 5 a and b). At the base of this sedimentary section, in the southwestern sector of the Meseta de Chalía, volcaniclastic rocks intercalated with tuff deposits reveal growth-strata geometries in both, the forelimb (Fig. 5d) and backlimb (Fig. 5f) of a west-vergent fold, indicating syncontractional deposition in this area. U-Pb geochronology on detrital zircons from these deposits yielded a late Eocene age (see following section).

Over the San Bernardo FTB, the late Oligocene/early Miocene within-plate mafic rocks that extend over the Cretaceous strata, preserve evidence of a synextensional control on their emplacement (Fig. 6a,b,c). In the Sierra de los Aisladores (see location in Fig. 2), a horst structure separates two small halfgraben depocenters filled with volcanic agglomerates and intercalated lava flows belonging to the late Oligocene/early Miocene Buen Pasto Formation (Fig. 6a). In particular, the eastern halfgraben preserves evidences of lava flows injected through fault planes (Fig. 6b). At the western flank of the San Bernardo FTB, a preserved extensional depocenter reveals a growth-wedge in volcanic agglomerates and lavas of the Buen Pasto Formation (Fig. 6c). Folding and thrusting of this unit are well recorded in the northwestern flank of the San Bernardo FTB, where several short wave-length anticlines (0.5-1.5 km) are

observed (Figs. 2 and 6d), and at the surroundings of the Buen Pasto locality where volcanic rocks dated between ~20-18 Ma (Bruni et al., 2008) are dislocated by a west verging thrust (Figs. 2 and 6e). In the southernmost area of the San Bernardo FTB, in the foothills of the Río Senguer anticline, 5ºW dipping platform sandstone deposits of the Neogene Suprapatagoniense beds (Figs. 2 and 6f) cover a chaotic mass of blocks composed of bioclastic medium-grained sandstones of variable sizes (~0.2-5 m^3) (Figs. 6g and h). The larger blocks are embedded in a bioclastic sandy matrix that contains poorly-sorted blocks of smaller sizes (Fig. 6h). The depicted features along with the appearance of some tightly folded blocks, possibly attest for slumping and debris-flow processes in underwater conditions (Fig. 6i). According to these characteristics, the studied deposits would correspond to olistostromes. Similar, deposits in equivalent sections have been recently reported to the west of the study area (Foix and Casal, 2016). The fact that all blocks come from the Suprapatagoniense beds (i.e. not exotic) allows us to classify this deposit as an endolistostrome. Taking into account the synorogenic nature of this unit in the San Bernardo FBT (Paredes et al., 2006), the proximity of studied outcrops to the Codo del Senguerr anticline thrust-front (Fig. 2) and the fact that this unit was deposited in a low-gradient platform, we favor a tectonic trigger for olistostrome deposition. Finally, neotectonic activity was recognized east of Buen Pasto locality (see Fig. 2), where sandstones of the Cretaceous Chubut Group have been thrusted over Quaternary alluvial deposits (Fig. 7). Additionally, the latter deposits are deformed in an east verging box-shaped fold (Fig. 7a). This structure presents well preserved evidence of syn-tectonic sedimentation as depicted by hinge migration-related geometries that outline a growth triangle (Fig. 7a). Immediately to the north, we found a tectonic contact between the Chubut Group and Quaternary strata through a reverse fault (Fig. 7b).

In summary, Eocene syncontractional growth-strata were found to the east and south of the San Bernardo FTB and further west over the Andean foothills at the Meseta de Chalía. Latest Oligocene to early Miocene synextensional volcano-sedimentary deposits, belonging to the Buen Pasto Formation, were described in different sectors over the San Bernardo FTB. In the southernmost area of this belt, olistostrome deposits in the synorogenic Suprapatagoniense beds were found next to the Río Senguer thrust. Finally, neotectonic structures have been identified affecting the eastern flank of the San Bernardo FTB.

4. U-Pb Geochronology

Heavy mineral concentrates of the <350 μm fraction from 3 rock samples were separated using traditional techniques at ZirChron LLC. Zircons from the non-magnetic fraction were mounted in a 1-inch diameter epoxy puck and slightly ground and polished to expose the surface and keep as much material as possible for laser ablation analyses. After cathode-luminescence (CL) imaging at University of Idaho, the LA-ICP-MS U-Pb analyses were conducted at Washington State University using a New Wave Nd:YAG UV 213-nm laser coupled to a Thermo Finnigan Element 2 single collector, double-focusing, magnetic sector ICP-MS. Operating procedures and parameters are similar to those of (Chang et al., 2006). Laser spot size and repetition rate were 30 microns and 10 Hz, respectively. He and Ar carrier gases delivered the sample aerosol to the plasma. Each analysis consists of a short blank analysis followed by 250 sweeps through masses 202, 204, 206, 207, 208, 232, 235, and 238, taking approximately 30 seconds. Time-independent fractionation was corrected by normalizing U/Pb and Pb/Pb ratios of the unknowns to the zircon standards (Chang et al., 2006). U and Th concentrations were monitored by comparing to NIST 610 trace element glass. Two zircon standards were used: Plesovice, with an age of 338 Ma (Sláma et al., 2008) and FC-1, with an age of 1099 Ma (Paces and Miller, 1993). Uranium-lead ages were calculated and plots generated using Isoplot (Ludwig, 2003). Frequency histograms, relative probability plots of U-Pb detrital zircon ages, and Tera–Wasserburg concordia diagrams of the analyzed samples can be found in Fig. 8. A summary of the analytical results is presented in supplementary table S1. To determine the maximum depositional ages we identify the youngest age group (more than three) overlapping within the error (Gehrels et al., 2006). Then, we calculated an age from this group using the Tuffzirc algorithm of Ludwing et al. (2003) and age errors were reported using the quadratic sum of the analytical error plus the total systematic error for the set of analyses (Gehrels et al,. 2008) (Fig. 8a).

Three samples from the previously described syntectonic sequences were collected for U-Pb geochronology on detrital zircons. At the Grande-Funes anticline (Fig. 4a), a tuff from the growth-strata in the top of the Koluel Kaike Formation yielded an age of 43.9±0.5 Ma (Fig. 8), constraining the top of the syntectonic deposition to the middle Eocene. We carried out a similar analysis on a tuff sample collected from the growth-strata in the Meseta de Chalía (Fig. 5f). This sample yielded an age of 39.9±0.6 Ma (Fig. 8) suggesting late Eocene syntectonic deposition in

the Patagonian Andes. Finally, a sandstone sample from the Suprapatagoniense beds was collected from the outcrops near the Codo del Senguer anticline (Fig. 6f), yielding a maximum depositional age of 17.4±0.3 Ma (Fig. 8). Older zircon populations are centered on ~30 Ma, probably indicating that the source corresponds to the volcano-sedimentary Sarmiento Group (Ré et al., 2010) that crops out in the southern part of the San Bernardo FTB (Fig. 8a). Another older zircon population is centered on ~117 Ma with the Chubut Group in the study area or the Divisadero Group in the Andes as potential sources (Suárez et al., 2009; 2014) (Fig. 8a). This indicates two active source regions at ~17 Ma, one located in the main Andes to the west and the other in the foreland zone to the east.

5. Balanced structural cross-section from the Andean foothills to the foreland zone at ~45ºS

In order to obtain a more accurate portrait of deformation and to provide a shortening estimation across the Andes at the studied latitudes, we constructed a balanced cross-section from the North Patagonian Andes to the San Bernardo FTB using the Move® software (Midland valley Exploration Ltd.) (Fig. 9). The balanced cross-section for the San Bernardo FTB area was partly constrained using surface structural and stratigraphic data from a previous study (Gianni et al., 2015a). In addition new field data obtained in this work, particularly in the western flank of the study area, were incorporated. There, several NNW-trending short wave-length folds (0.5-1.5 km) were recognized affecting the Oligocene/Miocene volcanic cover (Figs. 2 and 9c). Fault geometry at depth in this area was defined on the basis of a published seismic-reflection line (Gianni et al., 2015a) located 20 km to the north of the presented cross-section. We used a detachment depth of 22 km, similar to the depth proposed by Echaurren et al. (2016) in a regional cross-section at 43ºS. Based on the construction of lithospheric strength profiles in the Patagonian foreland, these authors detected the presence of a mechanical contrast between the upper and lower crust, which they considered as advantageous for the development of a basal detachment in the lower crust (Fig. 9b). To reconstruct the North Patagonian Andes area, we used the structural cross-section of Folguera and Iannizzotto (2004) and structural and stratigraphic data previously published as geometrical constraints (Ploszkiewicz and Ramos, 1977; Iannizzotto et al., 2004).

To restore the cross-section, we assumed deformation of homogeneous blocks and competent beds with variable thickness and used the flexural-slip unfold algorithm (Griffiths et al., 2002), appropriate for structures related to tectonic inversion and strata with lateral thickness variations. Different structural styles can be recognized across the analyzed Andean and extra-Andean domains:

To the west, the North Patagonian Andes foothills constitute a generally east-vergent dominated thrust system, characterized by a western thin-skinned sector related to short wave-length folds (2.5-1 km), detached at Early Cretaceous deposits, and an eastern thick-skinned sector with longer wave-length folds (5-3 km) associated with the tectonic inversion of Late Jurassic to Earliest Cretaceous depocenters of the Río Mayo Sub-basin (Clavijo, 1986; Folguera and Iannizzotto, 2004; Iannizzotto et al., 2004). To the east, the San Bernardo FTB stands as a doubly vergent thick-skinned belt, related to the inversion of Jurassic-Early Cretaceous half-grabens that produced long wave-length structures (8-12 km) (Peroni et al., 1995; Homovc et al., 1995).

Calculated shortening magnitudes do not exceed 7 km in a 224.46 km length section, representing only a 3.14 % of the initial length (Fig. 9d). This value should be considered a minimum estimate since some sectors of the Andes that absorbed contractional deformation to the west were not integrated. Noteworthy, this shortening is similar to values in the northern sector of the PBF (10.69 km equivalent to a 3.78%) documented by Echaurren et al. (2016). Such low values are common in broken foreland areas where shortening does not overcome 2-3% (e.g. Allmendinger and Jordan, 1986).

6. Estimation of effective elastic thickness in the PBF

Effective Elastic Thickness

To explore the spatial relation between contractional structures in the PBF and location of weak lithospheric zones, we elaborated a local high-resolution analysis of lithosphere rigidity (D) in Central Patagonia. For long-term geological loads, the lithosphere is considered to respond regionally by flexure (Watts, 2001). Thereby, the lithosphere is usually represented as an infinite two dimensional elastic plate overlying on a relatively fluid substrate (mantle). This model is used when the load is located far from the plate margin. Otherwise, a broken plate or semi-infinite plate is used when the load is near the plate margin (Watts, 2001; Turcotte and

Schubert, 2002). As our study area is located relatively far from the continental margin (550-600 km) an infinite plate model is considered. The flexure or bending of the lithosphere w(x) when applying a known load $q_a(x) = \rho_t g h(x)$ is described by Equation 1 (Watts, 2001; Turcotte and Schubert, 2002), being h(x) the topography, $(\rho_m - \rho_c)gw(x)$ the restitutive force (ρ_t, ρ_c, ρ_m, are the densities of the topographic masses above sea level, the continental crust and the upper mantle, respectively) and P the horizontal stress. P is considered zero in our analysis, as has been shown at these latitudes by Tassara (2003). A parameter equivalent to rigidity and more commonly used is the effective elastic thickness (T_e), related to D through Equation 2. T_e represents the portion of the lithosphere that behaves elastically, with standard values of Young modulus $E = 10^{11}$ Pa and the Poisson ratio $\nu = 0{,}25$ (e.g. Watts, 2001; Kirby and Swain, 2011).

$$D\frac{d^4w}{dx^4} + P\frac{d^2w}{dx^2} + (\rho_m - \rho_c)gw(x) = q_a(x) \quad \text{Equation 1}$$

$$D = \frac{E\,T_e^{\,3}}{12(1-\nu^2)} \quad \text{Equation 2}$$

As the load is three dimensional, the deflection will be given by w(x, y). In addition, rigidity of large regions is usually variable, being this last fact represented by D(x, y). In this sense, Equation 1 is modified according García et al. (2015), considering the horizontal stress equal to zero:

$$\nabla^2[D\nabla^2 w] - (1-\nu)\left[\frac{\partial^2 D}{\partial x^2}\frac{\partial^2 w}{\partial y^2} - 2\frac{\partial^2 D}{\partial x\,\partial y}\frac{\partial^2 w}{\partial x\,\partial y} + \frac{\partial^2 D}{\partial y^2}\frac{\partial^2 w}{\partial x^2}\right] + (\rho_m - \rho_c)gw(x,y) = q_a(x,y) \text{ Ecuation 4}$$

Considering D(x, y) as constant inside a small particular region, the last equation is modified as follows:

$$D\nabla^4 w + (\rho_m - \rho_c)gw(x,y) = q_a(x,y) \text{ Ecuation 5}$$

Then, working in wavenumber domain ($k = (k_x, k_y)$), after applying Fourier Transform, Equation 5 can be rewritten as:

$$W(k_x, k_y) = \frac{\rho_t}{\rho_m - \rho_c}\,\Phi_e(k)\,H((k_x, k_y) \quad \text{Equation 6}$$

where bold upper-case variables W and H, are the wavenumber domain representations of the deflection w(x, y) and the topography h(x, y), respectively. $\Phi_e(k)$ is defined through Equation 7 (Watts, 2001), being K the module of the vector k:

$$\Phi_e(k) = \left[\frac{D\,K^4}{(\rho_m - \rho_c)g} + 1\right]^{-1} \quad \text{Equation 7}$$

The effective elastic thickness was calculated using the python code of Soler (2015), following the ideas considered by García et al. (2016), where rift sedimentary basins are considered as a buried load in the infinite plate model. It requires several data inputs: the topography $h(x, y)$ (Sandwell and Smith, 2009), the sedimentary thickness ($h_s(x, y)$) of basin infilling (San Jorge Gulf Basin (SJGB)), the Bouguer anomaly and the input of values for different parameters (see Table 1).

The Bouguer anomaly data were obtained from the EIGEN-6C4 model, which combines terrestrial and satellite data (Förste et al., 2014). Then, it was corrected by the gravimetric effect of the sedimentary infill (BACS) since sediment density is lower than mean crust density. The gravity effect was calculated through the software Oasis montaj (www.geosoft.com) in wave number domain implementing the Parker algorithm (Parker, 1973), using the sedimentary thickness of the GSJB published by Jones et al. (2004) and a density contrast $(\rho_{up} - \rho_s)$ equal to 0.37 g/cm^3. Subsequently, this effect was subtracted from the Bouguer anomaly to obtain the BACS.

The methodology consists first, in calculating the deflection ($w_{inverter}$) of the lithosphere through the inversion of the BACS for the whole study area, using the Parker-Oldenberg algorithm (Parker, 1973; Oldenburg, 1974), considering a density contrast between upper mantle and lower crust ($\rho_m - \rho_{lc}$) equal to 0.44 g/cm^3. The code contains an interface that allows choosing windows with variable sizes and positions, being T_e constant inside each window. We used windows with sizes of 70x70km and 110x110km, which are optimum dimensions for a local T_e analysis (García et al., 2016). For any chosen window, several T_e values are considered and their respective deflections w_{local} calculated using Equation 6. Each w_{local} is calculated considering the topography load for the whole study area. Then, each one of these w_{local} is compared with the inverted gravimetric deflection ($w_{inverter}$) inside the chosen window and the reliable T_e value is that which presents the minimum rms (root mean square) between both. Finally, the T_e of a high density of windows resulted in a grid of variable T_e for the analyzed region (Fig. 10a).

Some important insights can be drawn from the obtained map in Fig. 10a. First, Te values are in general, low (<35 km) for most of the Central Patagonia (Fig. 10a). Lithosphere with such

low T_e values usually deforms involving deep-seated basement faults (Watts, 1995; Mouthereau et al., 2013), which correlates with the thick-skinned style of deformation described for most of the Patagonian Andes and the Patagonian broken foreland (Orts et al., 2012; Ghiglione et al., 2014; Bilmes et al., 2013; Echaurren et al., 2016; Giacosa et al., 2010).

Secondly, intraplate contraction does not seem to have situated randomly, but largely located on areas of lowest Te (<15 km) and hence, in those places where the lithospheric strength was lowest (Fig. 10a).

7. Discussion

7.1. Interpretation of field and geochronology data

Surface description of growth-strata in the upper Río Chico Group (Koluel Kaike Formation) and determination of an age of ~44 Ma for these deposits are indicative of the occurrence of Eocene intraplate tectonics in the San Bernardo FTB (Figs. 3, 4 and 8a). Notably, the age reported here for this unit is consistent with recent magnetostratigraphic and geochronological data that constrain the temporal span of the Koluel-Kaike Formation to the 46.7–42.2 Ma interval (Lutetian) (Krause et al., 2017). Additionally, the new documentation of the existence of Eocene deposits in the Meseta de Chalía dated in ~40 Ma and the finding of growth-strata in these rocks; indicate the presence of Eocene contraction in the cordilleran area (Figs. 5 and 8a). Notably, description of syntectonic sedimentation limited to the upper unit of the Río Chico Group allows further refining previous proposals based on scarce seismic reflection data (e.g. Paredes et al. 2006; Navarrete et al. 2015), that suggested a syntectonic origin for the totality of this group, implying contraction since late Paleocene. Altogether, the presented data would indicate that a contractional tectonic regime took place during Eocene times at studied latitudes. The presence of synextensional deposits related to mafic within-plate magmatism in the San Bernardo FTB validates previous interpretations of Oligocene/early Miocene extensional tectonics based on geochemical studies (e.g. Bruni et al., 2008) (Fig. 6a,b,c). The observation of folds and thrusts affecting the latter volcanic unit indicates a contractional reactivation of the San Bernardo FTB (Fig. 6d,e). This episode was possibly linked to synorogenic deposition of the shallow marine deposits as indicated by growth strata description in seismic reflection lines (Paredes et al., 2006). In the study area, this episode could

have triggered deposition of a sedimentary breccia interpreted as an olistostrome deposit in the Suprapatagoniense beds next to the Río Senguerr anticline (Fig. 6f). U-Pb dating on detrital zircons from these deposits allowed constraining this event to the early-middle Miocene (~17.4 Ma) (Fig. 8a). Finally, thrusts and folds in Quaternary alluvial deposits attest for an ongoing contractional regime in the study area (Fig. 7).

7.2. Cenozoic intraplate tectonic events in the PBF: Their relation to Andean phases

During the middle to late Eocene (~44-40 Ma), a contractional tectonic event was identified at the studied latitudes, which was recorded from the North Patagonian Andes to the PBF (Fig. 11). Noteworthy, the occurrence of uplift and exhumation during an approximately similar time interval (50-40 Ma) has been widely documented in the Northern (e.g. Restrepo-Moreno et al., 2009; Parra et al., 2009), Central (e.g. Cobbold and Rossello, 2003; Arriagada et al., 2006; Barnes and Elhers, 2009) and Southern Andes (e.g. Ramos, 2005 and references therein). Particularly, in the Central Andes this event is known as the Incaic orogenic phase (Steinmann, 1929). According to Charrier et al. (2007), this phase was responsible for the uplift of the Incaic ranges, an early expression of the Andean orogen. The southernmost record of this phase was described north of the study area in the Neuquén Basin (Cobbold and Rossello, 2003). In this context, recognition of Eocene contraction in this study constitutes an unprecedented register of this phase in Central Patagonia. However, a similar deformation stage is not described immediately to the north of the study area between 39ºS and 44ºS. In that area, an absence of record of exhumation in Eocene times has been determined from thermochronological studies (Savignano et al., 2016). It is worth noting that if burial was not important after the Cretaceous contractional event that characterized this region (e.g. Echaurren et al., 2016; Savignano et al., 2016), then Eocene deformation may not be registered in thermochronological data. Notably, Eocene contraction documented in this study, along with the record of coeval magmatic arc activity (Pankhurst et al., 1999) are indicative of ongoing subduction at this time, which contradicts previous proposals of a transform margin in Patagonia (Aragón et al., 2013).

During the Latest Oligocene, a switch to extensional intraplate deformation is observed in the study area (Fig. 11). This stage could have been related to an event of regional extension at this time that interrupted Andean orogenesis between 39ºS to 46ºS (e.g. Muñoz et al., 2000; see Encinas et al., 2015, for a synthesis). The causes of this extensional stage are under intense

discussion, existing a diversity of models to explain extension and intraplate magmatism (slab roll-back, Muñoz et al., 2000; mantle plume, Kay et al., 2006; asthenospheric upwelling, Bruni et al., 2008; slab window, Aragón et al., 2013; delamination, Remesal et al., 2012; changes in convergance rates, Jordan et al., 2001). According to Encinas et al. (2017) crustal thinning allowed the marine flooding of Patagonia reaching its maximum extension at ~20 Ma. It was followed by regional contraction that started around 19–16 Ma as indicated by fluvial synorogenic deposition related to the growth of the Patagonian Andes (Thomson, 2002; Lagabrielle et al., 2004; Orts et al., 2012). At this time, the PBF reactivated in the foreland zone achieving its full development (Fig. 11). Synchronic uplift along strike the PBF in middle Miocene is supported by our 17.4 Ma maximum age obtained for marine synorogenic deposits, similar to the age published by Bilmes et al. (2013) in the northern sector of the PBF (~16.1 Ma). Noteworthy, the obtained age for shallow marine rocks in the San Bernardo FTB has significant implications for the Neogene paleogeography of Patagonia, which is still debated (see Encinas et al., 2017 for a review). The presented ~17 Ma age for the Suprapatagoniense beds along with 19.6 to 15.3 Ma ages (Parras et al., 2012; Suárez et al., 2015; Cuitiño et al., 2016) for an equivalent unit immediately to the east of the study area (Chenque formation) in the eastern San Jorge Gulf Basin (Fig. 1), would indicate that, contrarily to what has been described in southern Patagonia, 1) there is a contemporaneity between fluvial synorogenic and shallow marine deposition and 2) the sea retired later from the study area. Furthermore, this age contradicts previous suggestions about the beginning of intraplate contraction at 15-10 Ma in the San Bernardo FTB (e.g. Peroni et al., 1995). The occurrence of Neogene contractional deformation is not unique to the PBF; it is a common feature to the whole Andean orogen that is generally attributed to the Quechua phase (Steinmann, 1929). Neotectonic evidence described in this work indicates that contractional activity is an ongoing process in the San Bernardo FTB. Thus, in Central Patagonia the Incaic and Quechua Andean phases produced deformation at an anomalous distance from the trench (550-600 km) that accommodated a subtle amount of shortening (3.14%) in the study area.

7.3. The role of lithospheric strength on intraplate deformation location

It is well known that active margins impart important forces on the edges of continental plates, often creating an associated intraplate stress field (e.g. Heidbach et al., 2008, Raimondo et al., 2014). However, intraplate deformation usually takes place in specific sectors of the foreland

lithosphere, which reflects exceptional conditions for this process to take place. Such conditions depend on a variety of factors (e.g. crustal heterogeneities, thermal weakening and fluid-rock interaction) that aid to weaken the lithosphere, enabling it to accommodate deformation (e.g. White et al., 1986; Sandiford and McLaren, 2002; Clarck et al., 2006). In this sense, the occurrence of intraplate contraction in the PBF has been attributed to the existence of a weak lithosphere in Central Patagonia that concentrated deformation during tectonic events (Bilmes et al., 2013; Gianni et al., 2015a; Echaurren et al., 2016). The high-resolution analysis of the effective elastic thickness presented in this work reveals that, in general, the whole Central Patagonia is characterized by a low lithospheric rigidity (Te<30km) (Fig. 10a). However, basement intraplate contractional structures localized preferentially in those areas characterized by the lowest rigidity values (Te<15 km) (Fig. 10a). Notably, low Te zones are roughly coincident with the location of previous late Paleozoic to Mesozoic intraplate rift basins (Uliana et al., 1989; Peroni et al., 1995; Homovc and Constantini, 2001; Figari, 2005) (Fig. 10a). Thus, it is likely that intraplate zones that experienced extension have thermo-mechanically weakened the lithosphere (Thomson, 2002; Fosdick et al. 2014), leaving them prone to absorb deformation in later contractional stages (e.g. Arnais-Rodríguez and Audemard, 2014). Notably, these basins have played a major role in building the PBF through positive inversion of favorably oriented NW- and NNW-trending normal faults (Giacosa et al., 2010; Bilmes et al., 2013; Gianni et al., 2015a; Huyghe et al., 2015). In addition, widespread Neogene contraction in Central Patagonia may have also been aided, at least secondarily, by thermal softening during the Paleogene, associated with eruptions of within-plate magmatism over Central Patagonia (e.g. Thompson et al., 2001) (Fig. 1c).

We suggest that the lack of similar intraplate deformation to the south of the study area is due to the presence of a different previous structural framework and of a distinct configuration of lithospheric strength in the southernmost Patagonian foreland. There, intraplate basins characterized by repeated rifting events, as documented in Central Patagonia, are absent. Instead, short-lived Jurassic extension focalized near the continental edge in a marginal basin, bounded by subsiding but almost undeformed platforms that produced a narrow plate-margin orogen during basin inversion (Kley et al., 1999; Ghiglione et al., 2014; 2016).

8. Conclusions

A multidisciplinary approach involving description of syntectonic deposits, U/Pb geochronology, structural modeling and calculation of effective elastic thickness allowed to better constrain intraplate deformation in the central sector of the PBF. During middle to late Eocene, contraction took place from the North Patagonian Andes to the intraplate sector in the PBF. Recognition of this event constitutes an unprecedented record of the Incaic phase in Central Patagonia. The tectonic regime changed to extension during late Oligocene/early Miocene, as indicated by the description of synextensional deposits in the San Bernardo FTB. From middle Miocene (~17 Ma) to present the tectonic regime switched back to contraction during the Quechua phase, reactivating intraplate deformation in the PBF. The elaboration of a high resolution analysis of the effective elastic thickness in Central Patagonia shows that intraplate contraction localized mainly in areas of lower lithospheric strength (Te<15 km). Hence, the observed strain distribution in the PBF appears to be largely controlled by lateral variations in the lithospheric strength. Variations in this parameter could be related to the Paleozoic-Mesozoic history of intraplate rifting that could have caused thermo-mechanical weakening of the foreland lithosphere. Finally, the Cenozoic evolution of the PBF could help to better understand deformation and lithospheric rheological conditions in ancient intraplate belts linked to similar Andean-type subduction settings.

9. Acknowledgements

This work was financed by PIP 11220110100506, UBACYT 20020110100019, PICT-2012-1490, Fondecyt projects 1110914 and 1151146 and the Consejo Nacional de Investigaciones Científicas y Técnicas (CONICET). We are grateful to Midland Valley Ltd. for providing the Academic Licenses of the Move software. The authors are thankful to Dr. Ulrich Riller and anonymous reviewers that provided critical and constructive comments on this and a previous version of this manuscript.

10. References

Aguirre Urreta, B., Ramos, V., 1981. Estratigrafía y paleontología de la alta cuenca de río Roble, Cordillera Patagónica. in 8th Congreso Geológico Argentino. Actas 3, pp. 101–138, Asoc. Geol. Arg., San Luis.

Aitken, A. R. A., Raimondo, T., Capitanio, F. A., 2013. The intraplate character of supercontinent tectonics. Gondwana Res. 24, 807–814. doi:10.1016/j.gr.2013.03.005.

Allard, J. O., Paredes, J. M., Foix, N., Giacosa, R. E., 2015. Conexión cretácica entre las cuencas del golfo San Jorge y cañadón Asfalto (Patagonia): paleogeografía, implicancias tectonoestratigráficas y su potencial en la exploración de hidrocarburos. Rev. la Asoc. Geol. Arg. 72, 21–37.

Jordan, T. E., Allmendinger, R. W., 1986. The Sierras Pampeanas of Argentina; a modern analogue of Rocky Mountain foreland deformation. Am. J. of Sci. 286, 737-764.

Arriagada, C. Cobbold, P. R., Roperch, P., 2006. Salar de Atacama basin: A record of compressional tectonics in the central Andes since the mid-Cretaceous. Tectonics 25.

Barcat, C., Cortiñas, J.S., Nevistic, V.A., Stach, N.H., Zucchi, H.E., 1984. Geología de la region comprendida entre los lagos Musters-Colhue Huapi y la Sierra Cuadrada. Departamento Sarmiento y Paso de Indios, Provincia del Chubut. In IX Geological congress of Argentina, Buenos Aires, 2. pp. 263–282.

Barnes, J. B., Ehlers, T. A., 2009. End member models for Andean Plateau uplift. Earth Sci. Rev. 97, 105-132.

Barreda, V., E., Bellosi, 2014. Ecosistemas terrestres del Mioceno Temprano de la Patagonia central, Argentina: primeros avances. Rev. del Mus. Argentino Ciencias Nat. nueva Ser. 5, 125–134.

Bilmes, A., D'Elia, L., Franzese, J. R., Veiga, G. D., Hernández, M., 2013. Miocene block uplift and basin formation in the Patagonian foreland: The Gastre Basin, Argentina, Tectonophysics 601, 98–111. doi:10.1016/j.tecto.2013.05.001.

Blisniuk, P. M., Stern, L. A., Chamberlain C. P., Idleman B., Zeitler, P. K.,2005. Climatic and ecologic changes during Miocene surface uplift in the Southern Patagonian Andes, Earth Planet. Sci. Lett. 230, 125–142. doi:10.1016/j.epsl.2004.11.015.

Brocher, T.M., 2005. Empirical relations between elastic wave speeds and density in the Earth's crust. Bull. Seismol. Soc. Am. 95, 2081-2092.

Bruni, S., D'Orazio, M., Haller, M. J., Innocenti, F., Manetti, P., Pécskay, Z., Tonarini, S., 2008. Time-evolution of magma sources in a continental back-arc setting: the Cenozoic basalts from Sierra de San Bernardo (Patagonia, Chubut, Argentina). Geol. Mag. 145, 714–732. doi:10.1017/S0016756808004949.

Chang, Z., Vervoort, J. D., McClelland, W. C., Knaack, C., 2006. U-Pb dating of zircon by LA-ICP-MS. Geochemistry, Geophys. Geosystems. 7. doi:10.1029/2005GC001100.

Charrier, R., Pinto, L., M., Rodríguez, P., 2007. Tectonostratigraphic evolution of the Andean Orogen in Chile, in: Moreno, T. and Gibbons, W. (Eds.), The geology of Chile, The geological Society, pp. 21-114.

Clarck, C., Hand, M., Faure, K., Mumm, A. S., 2006. Up-temperature flow of surface-derived fluids in the mid-crust: the role of pre-orogenic burial of hydrated fault rocks. J. Metamorph. Geol. 24, 367–387. doi:10.1111/j.1525-1314.2006.00643.x.

Clavijo, R., 1986. Estratigrafía del Cretácico Inferior en el sector occidental de la Cuenca del Golfo San Jorge. Boletín Inf. Pet. 9, 15–32.

Chulick, G.S., Detweiler, S., Mooney, W.D. 2013. Seismic structure of the crust and uppermost mantle of South America and surrounding oceanic basins. J. South Am. Earth Sci. 42, 260-276.

Cobbold, P. R., Rossello, E. A., 2003. Aptian to recent compressional deformation, foothills of the Neuquén Basin, Argentina. Mar. and Petr. Geol. 20, 429-443.

Cornaglia, L., Ruiz, F., Introcaso, A. 2009. Análisis cortical de la cuenca Golfo de SanJorge utilizando anomalías de Bouguer y ondulaciones delgeoide. Rev. Asoc. Geol. Arg. 65, 504-515.

Cuitiño, J.I., Scasso, R.A., Ventura, Santos, R., Mancini, L.H., 2015. Sr ages for the Chenque Formation in the Comodoro Rivadavia region (Golfo San Jorge Basin, Argentina): stratigraphic implications. Lat. Am. J. of Sed. and Bas. An. 22, 3-12.

Cunningham, D., 2005. Active intracontinental transpressional mountain building in the Mongolian Altai: defining a new class of orogen. Earth Planet. Sci. Lett. 240, 436–444.

Dal Molin, C., Franchi M., 1996. Reinterpretación estratigráfica de las sedimentitas terciarias del sudoeste de Chubut. In: Actas XIII Congreso Geológico Argentino, vol. 1, pp. 473–478, Mendoza.

Dickinson, W. R., Snyder, W. S., 1978. Plate tectonics of the Laramide orogeny. Geol. Soc. Am. Mem. 151, 355–366.

Duff, B. A., Langworthy, A. P., 1974. Orogenic zones in central Australia: intraplate tectonics?. Nature. 249, 645–647. doi:10.1038/249645a0.

Echaurren, A., Folguera, A., Gianni, G.M., Orts, D., Tassara, A., Encinas, A., Valencia, V., 2016. Tectonic evolution of the North Patagonian Andes (41°–44° S) through recognition of syntectonic strata. Tectonophysics. 677, 99-114.

Echaurren, A., Oliveros, V., Folguera, A., Ibarra, F., Creixell, C., Lucassen, F., 2017. Early Andean tectonomagmatic stages in north Patagonia: insights from field and geochemical data. J. Geol. Soc. jgs2016-087.

Encinas, A., Folguera, A., Oliveros, V., De Girolamo Del Mauro, L., Tapia, F., Riffo, R., Hervé, F., Finger, K. L., Valencia, V. A., Gianni, G. M., Álvarez, O., 2015. Late Oligocene–Early Miocene submarine volcanism and deep marine sedimentation in an extensional basin of southern Chile: implications on the tectonic development of the North Patagonian Andes, Geol. Soc. Am. Bull. 128, 807-823.

Encinas, A., Folguera, A., Bechis, F., Finger, K. L., Zambrano, P., Pérez, F., Bernabé, P., Tapia, F., Riffo, R., Buatois, L., Orts, D., Nielsen, S. N., Valencia, V., Cuitiño, J., Oliveros, V., De Girolamo Del Mauro, L., Ramos, V. 2017. The late Oligocene-early Miocene marine transgression of Patagonia. In: Folguera et al. (Eds.), The making of the chilean-argentinian Andes, Springer, Berlin.

Fennell, L.M., Folguera, A., Naipauer, M., Gianni, G.M., Rojas Vera, E.A., Bottesi, G., Ramos, V.A., 2015. Cretaceous deformation of the Southern Central Andes: synorogenic growth strata in the Neuquén Group (35º 30′–37º S). Bas. Res. doi: 10.1111/bre.12135

Figari, E., 2005. Evolución tectónica de la cuenca de Cañadón Asfalto (zona del Valle Medio del Rio Chubut). Phd Thesis, Universidad Nacional de Buenos Aires. Facultad de Ciencias Exactas y Naturales, p. 198.

Figari, E. G., Strelkov, E., Laffitte, G., Cid De La Paz, M. S., Courtade, S.F., Celaya, J., Vottero, A., Lafourcade, P., Martinez, Villar, H., 1999. Los Sistemas Petroleros de la Cuenca del Golfo San Jorge: Sintesis Estructural, Estratigrafía y Geoquímica. in: Actas IV Congreso de Exploración y Desarrollo de Hidrocarburos, pp. 197–237, Mar del Plata.

Fitzgerald, M.G., Mitchum, R. M. Jr., Uliana, M., Biddle, K. T. A., 1990. Evolution of the San Jorge Basin, Argentina. Am. Assoc. Pet. Geol. Bullettin 74, 879–920.

Flint, S. S., Prior, D. J., Agar, S. M., Turner, P., 1994. Stratigraphic and structural evolution of the Tertiary Cosmelli Basin and its relationship to the Chile triple junction. J. Geol. Soc. London. 151, 251–268. doi:10.1144/gsjgs.151.2.0251.

Foix, N., Paredes, J. M., Giacosa, R. E., 2013. Fluvial architecture variations linked to changes in accommodation space: Río Chico Formation (Late Paleocene), Golfo San Jorge basin, Argentina. Sediment. Geol. 294, 342–355. doi:10.1016/j.sedgeo.2013.07.001.

Foix, N., G., Casal, 2016. Olistostromas en la Formación Chenque (Mioceno temprano), cuenca del golfo San Jorge: nuevas evidencias de actividad tectónica sinsedimentaria. In: IV jornadas de las ciencias de la Tierra "Dr. Eduardo Musacchio", Electronic book, Chubut, Argentina.

Fosdick, J. C., Graham, S. A., Hilley, G. E., 2014. Influence of attenuated lithosphere and sediment loading on flexure of the deep-water Magallanes retroarc foreland basin, Southern Andes. Tectonics. 33. doi:10.1002/2014TC003684.

Folguera, A., Iannizzotto, N. F., 2004. The lagos La Plata and Fontana fold-and-thrust belt: long-lived orogenesis at the edge of western Patagonia. J. South Am. Earth Sci. 16, 541–566. doi:10.1016/j.jsames.2003.10.001.

Förste, C., Bruinsma, S.L., Abrikosov, O., Lemoine, J-M, Marty J.C., Flechtner F., Balmino G., Barthelmes F., Biancale R. 2014. EIGEN-6C4 The latest combined global gravity field model including GOCE data up to degree and order 2190 of GFZ Potsdam and GRGS Toulouse. GFZ Data Services. http://doi.org/10.5880/icgem.2015.1.http://icgem.gfzpotsdam.de/ICGEM/ICGEM.html

García H., Soler S., Gianni, G.M., Ruiz. F., 2016. Análisis flexural de la cuenca Cretácico-Paleógena del noroeste Argentino. La subcuenca Lomas de Olmedo: zona de transición entre dos mecanismos de deformación distintivos. Primer Simposio de Tectónica Sudamericana. Chile.

García Morabito, E., Ramos, V.A., 2012. Andean evolution of the Aluminé fold and thrust belt, Northern Patagonian Andes (38°300–40°300S). J. S. Am. Earth. Sci. 38,13–30

Gehrels, G. E., Valencia, V.A., Pullen, A., 2006. Detrital zircon geochronology by laser-ablation multicollector ICPMS at the Arizona LaserChron Center. Pal. Soc. Papers. 12, 67.

Gehrels, G. E., Valencia, V. A., Ruiz, J., 2008. Enhanced precision, accuracy, efficiency, and spatial resolution of U-Pb ages by laser ablation–multicollector–inductively coupled plasma–mass spectrometry. Geochemistry, Geophys., Geosystems 9(3).

Ghiglione, M. C., Likerman, J., Barberón, V., Beatriz Giambiagi, L., Aguirre-Urreta, B., Suarez, F., 2014. Geodynamic context for the deposition of coarse-grained deep-water axial channel systems in the Patagonian Andes. Bas. Res. 26, 726-745.

Ghiglione, M. C., 2016. Orogenic Growth of the Fuegian Andes (52–56) and Their Relation to Tectonics of the Scotia Arc. In: Folguera et al. (Eds.), Growth of the Southern Andes, , Springer International Publishing, pp. 241-267.

Giacosa, R., Zubia, M., Sánchez, M., Allard, J., 2010. Meso-Cenozoic tectonics of the southern Patagonian foreland: Structural evolution and implications for Au–Ag veins in the eastern Deseado Region (Santa Cruz, Argentina). J. South Am. Earth Sci. 30,134–150. doi:10.1016/j.jsames.2010.09.002.

Gianni, G.M., Navarrete, C., Orts, D., Tobal, J., Folguera, A., Giménez, M., 2015a. Patagonian broken foreland and related synorogenic rifting: The origin of the Chubut Group Basin, Tectonophysics 649, 81–99. doi:10.1016/j.tecto.2015.03.006.

Gianni, G. M., Navarrete, C. G., Folguera, A., 2015b. Synorogenic foreland rifts and transtensional basins: A review of Andean imprints on the evolution of the San Jorge Gulf, Salta Group and Taubaté Basins. J. South Am. Earth Sci. doi:10.1016/j.jsames.2015.08.004.

González, R. R. L., 1978. Descripción geológica de las hojas 49a, Lago Blanco y 49b, Paso Río Mayo, in Provincia del Chubut, vol. 154, pp. 1–45, Servicio Geológico Nacional, Buenos Aires.

Griffiths, P., Jones, S., Salter, N., Schaefer, F., Osfield, R., Reiser, H., 2002. A new technique for 3-D flexural-slip restoration. J. Struct. Geol. 24,773–782. doi:10.1016/S0191-8141(01)00124-9.

Hamilton, W. B., 1988. Laramide crustal shortening. Geol. Soc. of Am. Mem. 171, 27-40.

Heidbach, O., Tingay, M., Barth, A., Reinecker, J., Kurfeß, D., Müller, B., 2008. The World Stress Map Database Release 2008. http://dx.doi.org/10.1594/GFZ.WSM.Rel2008.

Hinze, W.J., 2003. Bouguer reduction density, why 2.67?: Geophysics 68, 1559-1560.

Homovc, J. F., Constantini, L., 2001. Hydrocarbon exploration potential within intraplate shear-related depocenters: Deseado and San Julián basins, southern Argentina. Am. Assoc. Pet. Geol. Bull. 85, 1795–1816.

Homovc, J., Conforto, G., Lafourcade, P., Chelotti L., 1995. Fold Belt in the San Jorge Basin, Argentina: an Example of Tectonic Inversion, in: P. Buchanan, and J., Buchanan (Eds.), Basin Inversion, Geological Society Special Publication, pp. 235–248.

Horton, B. K., Perez, N. D., Fitch, J. D., Saylor, J. E., 2015. Punctuated shortening and subsidence in the Altiplano Plateau of southern Peru: Implications for early Andean mountain building. Lithosphere 7, 117-137.

Huyghe, D., Bonnel, C., Nivière, B., Fasentieux, B., Hervouët, Y., 2015. Neogene tectonostratigraphic history of the southern Neuquén basin (39°-40°30′S, Argentina): implications for foreland basin evolution. Basin Res. 27, 613–635. doi:10.1111/bre.12091.

Iannizzotto, N. F., Folguera, A., Leal, P. R., 2004. Control tectónico de las secuencias volcaniclásticas neocomianas y paleogeografía en la zona del Lago La Plata (45^{o}S). Sector interno de la faja plegada y corrida de los lagos La Plata y Fontana. Rev. la Asoc. Geológica Argentina 59, 655–670.

Introcaso, A., 2006. Geodesia física. Instituto de Fisiografía y Geología" Dr. Alfredo Castellanos".

Jones, S. M., White, N., Faulkner, P., Bellingham, P., 2004. Animated models of extensional basins and passive margins. Geochemistry, Geophys., Geosystems 5.

Jordan, T. E., Burns, W. M., Veiga, R., Pángaro, F., Copeland, P., Kelley, S., Mpodozis, C. 2001. Extension and basin formation in the southern Andes caused by increased convergence rate: A mid-Cenozoic trigger for the Andes. Tectonics 20,308–324. doi:10.1029/1999TC001181.

Kay, S. M., Ardolino, A. A., Gorring, M. L., Ramos, V. A., 2006. The Somuncura Large Igneous Province in Patagonia: Interaction of a Transient Mantle Thermal Anomaly with a Subducting Slab. J. Petrol. 48, 43–77. doi:10.1093/petrology/egl053.

Kirby, J. F., Swain, C. J., 2011. Improving the spatial resolution of effective elastic thickness estimation with the fan wavelet transform. Computers & geosciences 37, 1345-1354.

Klepeis, K., Betka, P, Clarke, G., Fanning, M., Hervé, F., Rojas, L., Mpodozis, C., Thomson, S. 2010. Continental underthrusting and obduction during the Cretaceous closure of the Rocas Verdes rift basin, Cordillera Darwin, Patagonian Andes. Tectonics 29. doi:10.1029/2009TC002610.

Kley, J., Monaldi, C. R., Salfity, J. A., 1999. Along-strike segmentation of the Andean foreland: causes and consequences. Tectonophysics 301, 75–94. doi:10.1016/S0040-1951(98)90223-2.

Krause, J. M., Clyde, W. C., Ibañez-Mejía, M., Schmitz, M. D., Barnum, T., Bellosi, E. S., Wilf, P., 2017. New age constraints for early Paleogene strata of central Patagonia, Argentina: Implications for the timing of South American Land Mammal Ages. Geol. Soc. Am. Bull. B31561-1.

Lagabrielle, Y., Suárez, M., Rossello, E., Hérail, G., Martinod J., Régnier´´ M., de la Cruz R., 2004. Neogene to Quaternary tectonic evolution of the Patagonian Andes at the latitude of the Chile Triple Junction. Tectonophysics 385, 211–241. doi:10.1016/j.tecto.2004.04.023.

Ludwig, K. R., 2003. ISOPLOT 3.0, a geochronological toolkit for microsoft excel. Berkeley Geochronology Center Special publication, no. 4, Berkeley.

Soler, S. R., 2015. Métodos Espectrales para la Determinación de la Profundidad del Punto de Curie y el Espesor Elástico de la Corteza Terrestre. Magister thesis.

Mouthereau, F., Watts, A. B., Burov, E., 2013. Structure of orogenic belts controlled by lithosphere age. Nat. geosc. 6, 785-789.

Muñoz, J., Troncoso, R., Duhart, P., Crignola, P., Farmer, L., Stern, C. R., 2000. The relation of the mid-Tertiary coastal magmatic belt in south-central Chile to the late Oligocene increase in plate convergence rate. Rev. geológica Chile 27. doi:10.4067/S0716-02082000000200003.

Navarrete, C. R., Gianni, G. M., Folguera, A., 2015. Tectonic inversion events in the western San Jorge Gulf Basin from seismic, borehole and field data. J. South Am. Earth Sci. 64, 486-497.

Oldenburg, D. W., 1974. The inversion and interpretation of gravity anomalies. Geophysics 39, 526-536.

Orts, D. L., Folguera, A., Encinas, A., Ramos, M., Tobal, J., Ramos, V. A., 2012. Tectonic development of the North Patagonian Andes and their related Miocene foreland basin (41°30′-43°S). Tectonics 31. TC3012, doi:10.1029/2011TC003084.

Pankhurst, R.J., Leat, P.T., Sruoga, P., Rapela, C.W., Márquez, M., Storey, B. C., Riley, T. R. 1998. The Chon Aike province of Patagonia and related rocks in West Antarctica: a silicic large igneous province. J. Volcanol. Geotherm. Res. 81,113–136.

Paces, J. B., Miller, J. D., 1993. Precise U-Pb ages of Duluth complex and related mafic intrusions, northeastern Minnesota: Geochronological insights to physical, petrogenetic, paleomagnetic, and tectonomagmatic processes associated with the 1.1 Ga midcontinent rift system. J. Geophys. Res. Solid Earth 98, 13997–14013.

Paredes, J.M., Azpiroz, G., Foix, N., 2006. Tertiary tectonics and sedimentation in the Cerro Piedra Oil Field Golfo San Jorge basin, Argentina. In: IV Latin American Congress of Sedimentology, Abstract, San Carlos de Bariloche, Argentina, p. 163.

Parker, R. L., 1973. The rapid calculation of potential anomalies. Geophys. J. Int. 31, 447-455.

Parra, M., Mora, A., Sobel, E. R., Strecker, M. R., González, R., 2009. Episodic orogenic front migration in the northern Andes: Constraints from low-temperature thermochronology in the Eastern Cordillera, Colombia. Tectonics 28.

Parras, A., Dix, G.R., Griffin, M., 2012. Sr-isotope chronostratigraphy of Paleogene/Neogene marine deposits: Austral Basin, southern Patagonia (Argentina). J. S. Am. Earth Sci. 37, 122-135.

Peroni, G. O., Hegedus, A. G., Cerdan, J., Legarreta, L., Uliana, M. A., 1995. Hydrocarbon Accumulation in an Inverted Segment of the Andean Foreland : San Bernardo Belt , Central Patagonia, in: H. J. Tankard et al., (Eds.), Petroleum Basins of South America, pp. 403–419.

Pérez Gussinyé, M., Swain, C. J., Kirby, J. F., Lowry, A. R., 2009. Spatial variations of the effective elastic thickness, Te, using multitaper spectral estimation and wavelet methods: examples from synthetic data and application to South America. Geochemistry, Geophys. Geosystems 10. doi:10.1029/2008GC002229

Ploszkiewicz, J. V, Ramos, V. A., 1977. Estratigrafía y tectónica de la Sierra de Payaniyeu (Provincia del Chubut), Rev. la Asoc. Geológica Argentina 32, 209–226.

Raigemborn, M. S., Krause, J. M., Bellosi, E., Matheos, S. D., 2010. Redefinición estratigráfica del grupo Río Chico (Paleógeno Inferior), en el norte de la cuenca del golfo San Jorge, Chubut. Rev. la Asoc. Geológica Argentina 67, 239–256.

Raimondo, T., Hand, M., Collins,W. J., 2014. Compressional intracontinental orogens: Ancient and modern perspectives, Earth-Science Rev. 130, 128–153, doi:10.1016/j.earscirev.2013.11.009.

Ramos, V. A., Cristallini, E. O., Pérez, D. J., 2002. The Pampean flat-slab of the Central Andes, J. South Am. Earth Sci. 15, 59–78. doi:10.1016/S0895-9811(02)00006-8.

Ramos, V. A., 2005. Seismic ridge subduction and topography: Foreland deformation in the Patagonian Andes. Tectonophysics 399, 73–86, doi:10.1016/j.tecto.2004.12.016.

Ré, G.H., Bellosi, E.S., Heizler, M., Vilas, J.F., Madden, R.H., Carlini, A.A., Kay, R.F., Vucetich, M.G., 2010. A geochronology for the Sarmiento Formation at Gran Barranca, in Madden, R.H. et al., (Eds.), The Paleontology of Gran Barranca: Evolution and Environmental Change through the Middle Cenozoic of Patagonia, Cambridge, UK, Cambridge University Press, p. 46–60.

Remesal, M. B., Salani, F. M., Cerredo, M. E., 2012. Petrología del complejo volcánico Barril Niyeu (Mioceno inferior), Patagonia Argentina. Rev. mex. cienc. geol. 29, 463-477.

Restrepo-Moreno, S. A., Foster, D. A., Stockli D. F., Parra-Sánchez, L. N., 2009, Long-term erosion and exhumation of the "Altiplano Antioqueño", Northern Andes (Colombia) from apatite (U–Th)/He thermochronology. Earth Planet. Sci. Lett. 278, 1-12.

Riba, O., 1976. Syntectonic unconformities of the Alto Cardener, Spanish Pyrenees: a genetic interpretation. Sed. Geol. 15, 213-233.

Savignano, E., Mazzoli, S., Arce, M., Franchini, M., Gautheron, C., Paolini, M., & Zattin, M. 2016. (Un) Coupled thrust belt-foreland deformation in the northern Patagonian Andes: new insights from the Esquel-Gastre sector (41° 30'–43° S). Tectonics.

Sciutto, J.C., 1981. Geología del Codo del Río Senguerr, Chubut, Argentina. In VIII Congreso Geológico Argentino, Actas 3. San Luis.

Sciutto, J., Césari, C., Lantanos, N., 2008. Hoja Geológica 4569-IV Escalante, provincia de Chubut. Inst. Geol. Recur. Miner. Serv. Geol. Min. Argent. Bol. 71.

Sandiford, M., S., McLaren, 2002. Tectonic feedback and the ordering of heat producing elements within the continental lithosphere. Earth Planet. Sci. Lett. 204, 133–150. doi:10.1016/S0012-821X(02)00958-5.

Sandwell, D.T., Smith, W.H., 2009. Global marine gravity from retracked Geosat and ERS-1 altimetry: Ridge segmentation versus spreading rate. J. Geoph. Res. 1978-2012, 114, B01411.

Sláma, J. et al. (2008). Plešovice zircon — A new natural reference material for U–Pb and Hf isotopic microanalysis. Chem. Geol. 249, 1–35. doi:10.1016/j.chemgeo.2007.11.005.

Steinmann G. 1929. Geologie von Peru. Karl Winter, Heidelberg (448 pp.)

Suárez, M., Márquez, M., 2007. A Toarcian retro-arc basin of Central Patagonia (Chubut), Argentina: Middle Jurassic closure,arc migration and tectonic setting. Rev. geológica Chile 34. doi:10.4067/S0716-02082007000100004.

Suárez, M., De La Cruz, R., Bell, M., Demant, A., 2009. Cretaceous slab segmentation in southwestern Gondwana. Geol. Mag. 147, 193, doi:10.1017/S0016756809990355.

Suárez M, Márquez M., De La Cruz, R., Navarrete, C., Fanning, M., 2014. Cenomanian-? Early Turonian Minimum Age of the Chubut Group, Argentina: SHRIMP U-Pb geochronology. J South Am Earth Sci 50,64-74.

Suárez, M., de la Cruz, R., Etchart, H., Márquez, M., Fanning, M. 2015. Síntesis de la Cronología Magmática Meso-Cenozoica de Patagonia Central, Aysén, Chile: edades U-Pb SHRIMP. XIV Congreso Geológico Chileno, ST-4: 789-792.

Tassara, A., Yáñez, G., 2003. Relación entre el espesor elástico de la litosfera y la segmentación tectónica del margen andino (15-47 S). Rev. Geol. Chile 30, 159-186.

Tassara, A., Echaurren, A., 2012. Anatomy of the Andean subduction zone: three-dimensional density model upgraded and compared against global-scale models. Geophys. J. Int. 189, 161–168. doi:10.1111/j.1365-246X.2012.05397.x.

Thompson, A. B., Schulmann, K., Jezek, J., Tolar, V., 2001. Thermally softened continental extensional zones (arcs and rifts) as precursors to thickened orogenic belts. Tectonophysics 332, 115–141, doi:10.1016/S0040-1951(00)00252-3.

Thomson, S. N., 2002. Late Cenozoic geomorphic and tectonic evolution of the Patagonian Andes between latitudes 42°S and 46°S: An appraisal based on fission-track results from the transpressional intra-arc Liquiñe-Ofqui fault zone. Bull. Geol. Soc. Am. 114, 1159–1173. doi:10.1130/0016-7606(2002)114<1159:LCGATE>2.0.CO;2.

Turcotte, D. L., Schubert, G., 2002. Geodynamics, Cambridge University Press. New York.

Uliana, M. A., Biddle, K. T., Cerdan, J., Tankard, A. J., Balkwill, H. R., 1989. Mesozoic extension and the formation of Argentine sedimentary basins the Atlantic margins, in: H. J.Tankard (Ed.), Extensional tectonics and stratigraphy, pp. 599–614, American Association of Petroleum Geologists, Tulsa, Oklahoma.

Watts, A. B., 2001. Isostasy and Flexure of the Lithosphere. Cambridge University Press.

Watts, A. B., Lamb, S. H., Fairhead, J. D., Dewey, J. F., 1995. Lithospheric flexure and bending of the Central Andes. Earth Planet. Sci. Let. 134, 9-21.

White, S. H., Bretan, P. G., Rutter, E. H., 1986. Fault-Zone Reactivation: Kinematics and Mechanisms, Philos. Trans. R. Soc. A Math. Phys. Eng. Sci. 317, 81–97. doi:10.1098/rsta.1986.0026.

Xu, Y. J., Cawood, P. A., Du, Y. S., 2016. Intraplate orogenesis in response to Gondwana assembly: Kwangsian Orogeny, South China. Am. J. of Sci. 316, 329-362.

Yang, Y., Liu, M., 2009. Crustal thickening and lateral extrusion during the Indo-Asian collision: a 3D viscous flow model. Tectonophysics 465, 128–135.

Ziegler, P. A., van Wees, J.D., Cloetingh, S., 1998. Mechanical controls on collision-related compressional intraplate deformation. Tectonophysics 300, 103–129. doi:10.1016/S0040-1951(98)00236-4

FIGURES

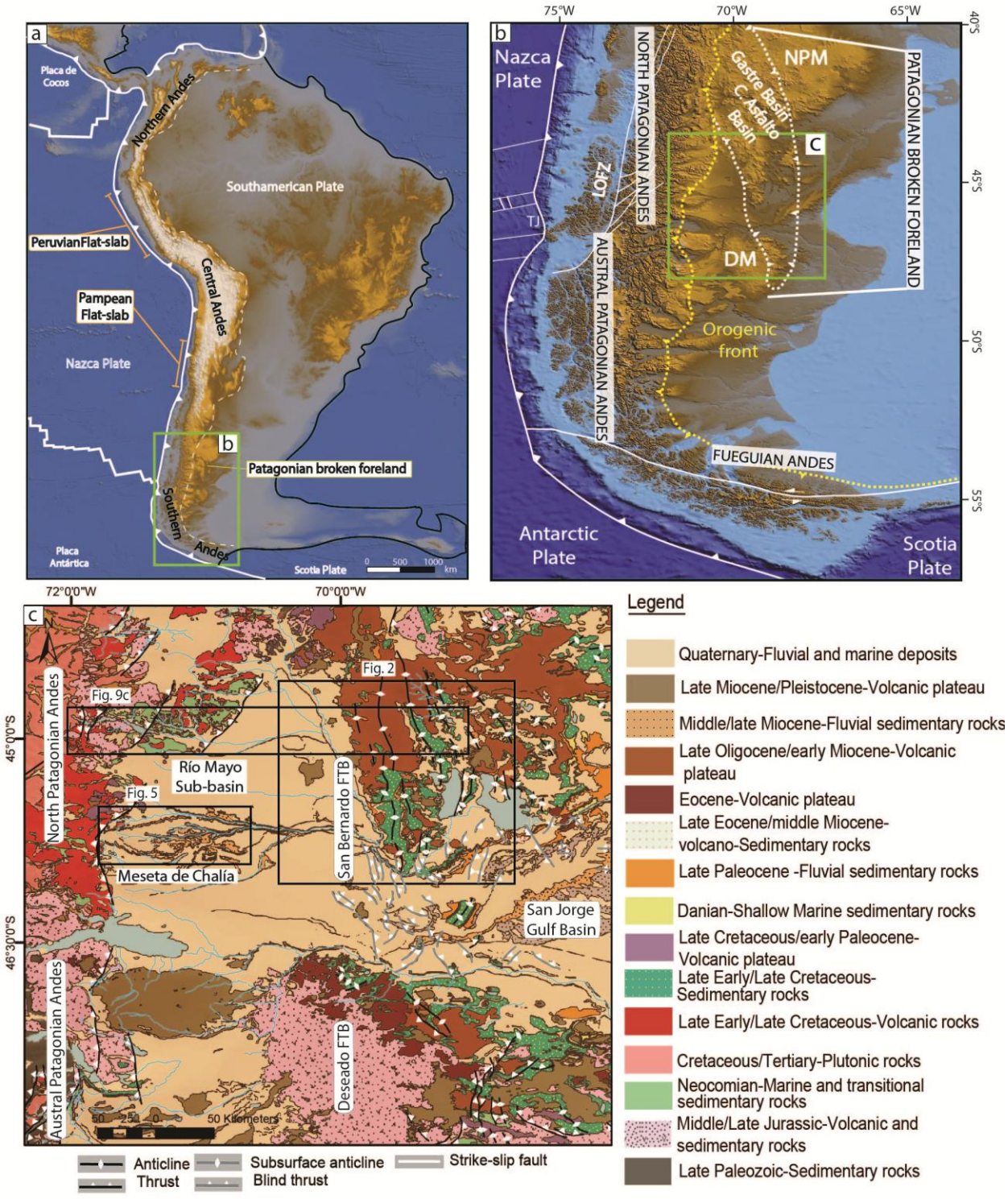

Fig. 1. (a) Tectonic setting of the Andes. (b) Tectonic setting of Patagonia showing the Patagonian Andes, the broken foreland area and location of map c). Abbreviations are TJ: Triple junction, LOFZ: Liquiñe-Ofqui fault zone, DM: Deseado Massif and NPM: North Patagonian Massif. (c) Geological sketch map showing the main sedimentary and morphostructural units

from Patagonia between ~44° to 48°S. Based on Giacosa et al. (2010), Ploszkiewicz and Ramos (1977), Dal Molin and Franchi (1996), Barcat et al. (1984) and Bruni et al. (2008).

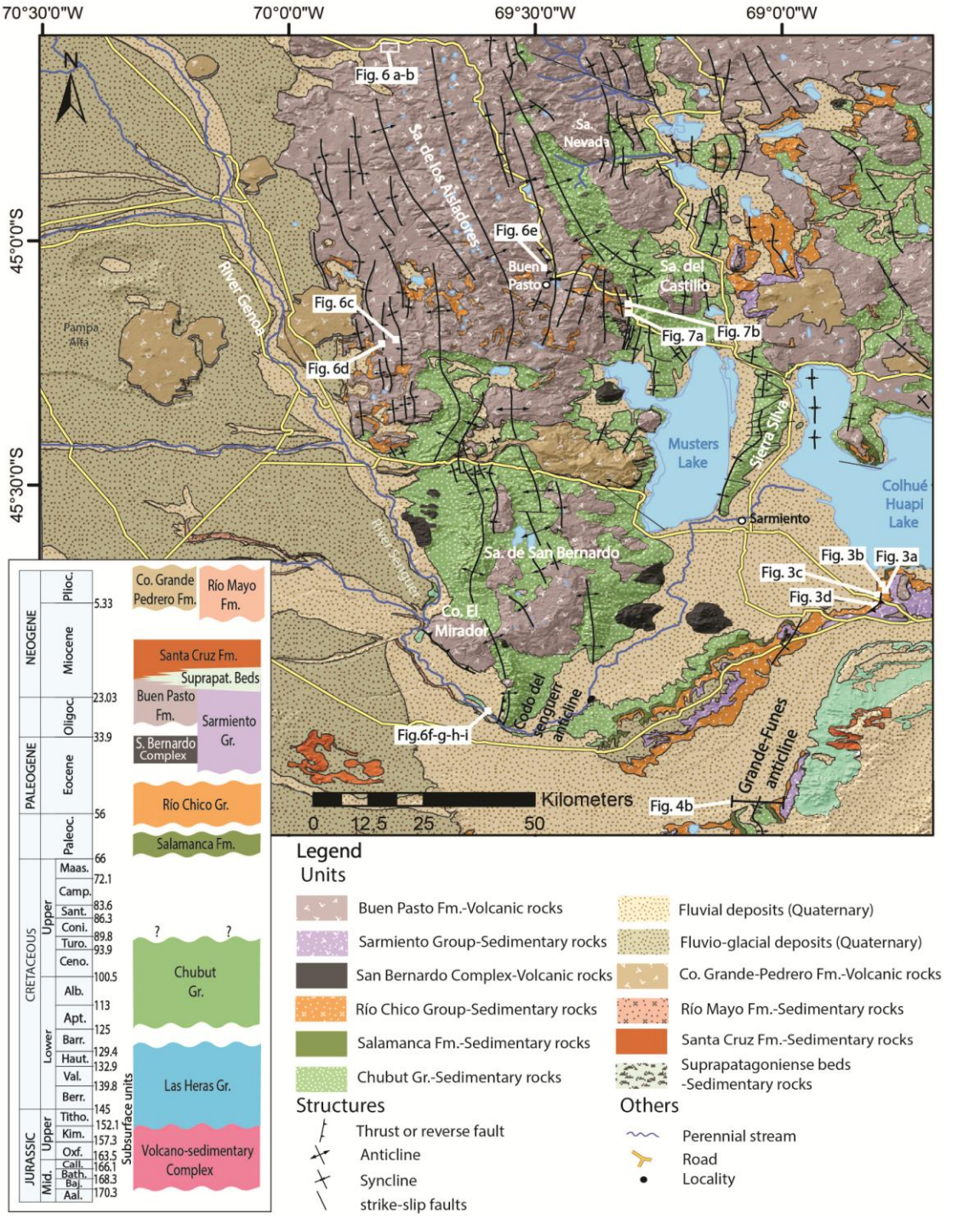

Fig. 2. Geological sketch map and stratigraphic chart of the San Bernardo FTB. Based on Sciutto (1981; 2008), Barcat et al. (1984), Bruni et al. (2008) and Gianni et al. (2015a). Structural mapping in the northwestern quadrant is from this work.

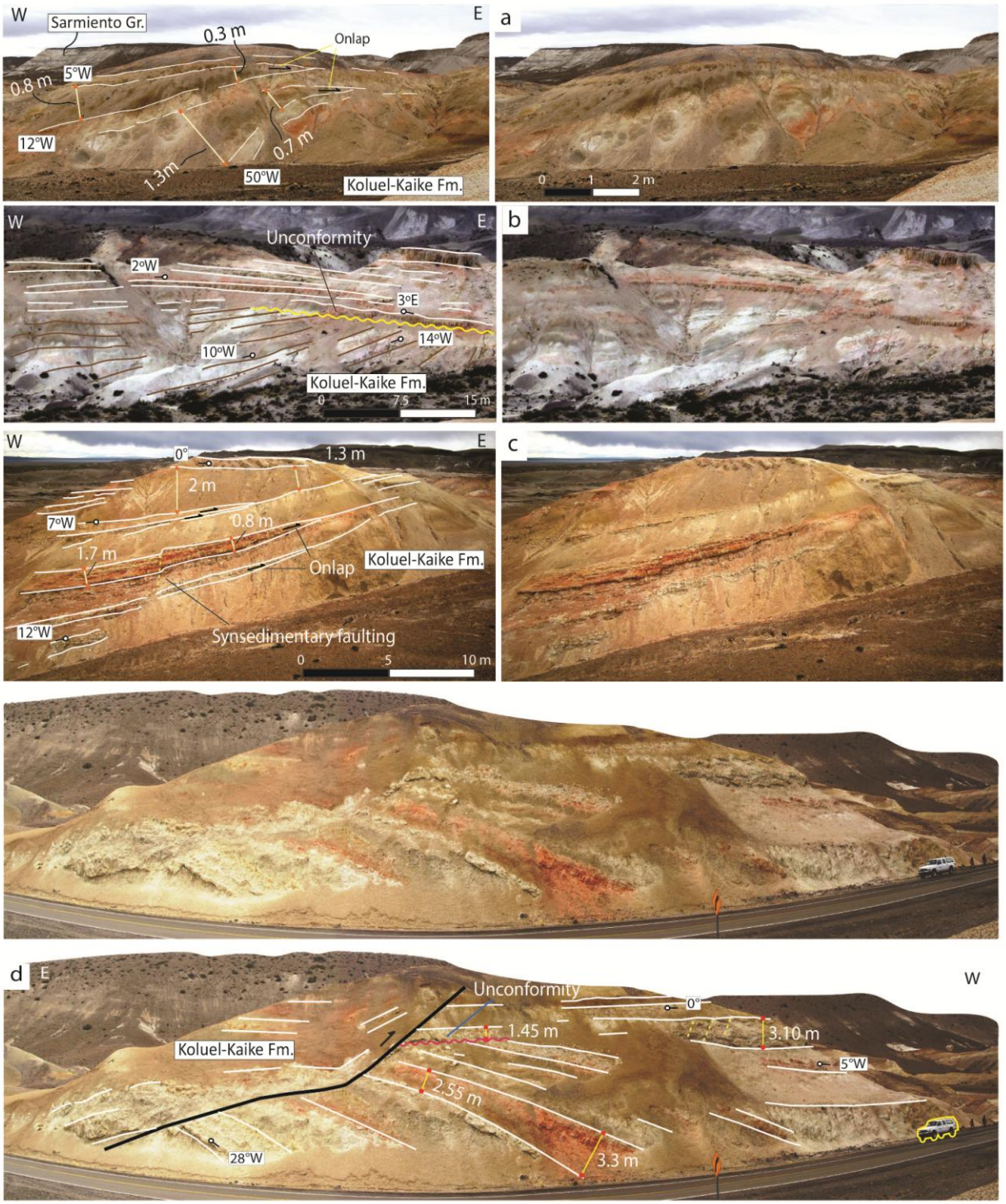

Fig. 3. (a) Growth fold in the upper Río Chico Group (Koluel Kaike Formation). (b)-(c) Growth-strata in the same unit. (d) Thrust-growth related to a detaching sheet in the Koluel Kaike Formation.

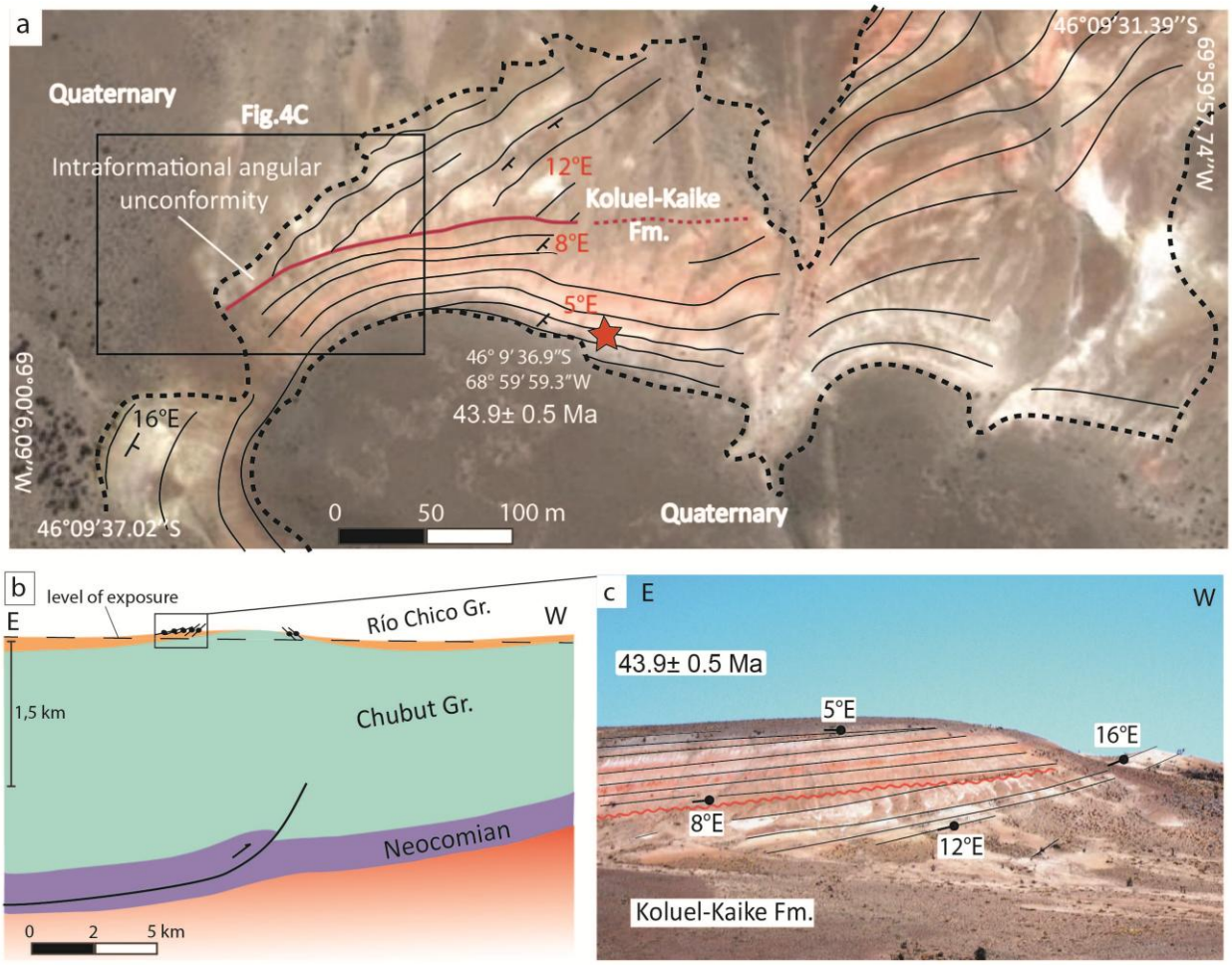

Fig. 4. (a) Map view of growth-strata in the Koluel Kaike Formation. (b) Schematic structural cross section at the Grande-Funes anticline from Fitzgerald et al. (1990) based on seismic reflection data. See section location in Fig. 2. (c) Growth-strata in the Koluel Kaike Formation at the Grande-Funes anticline.

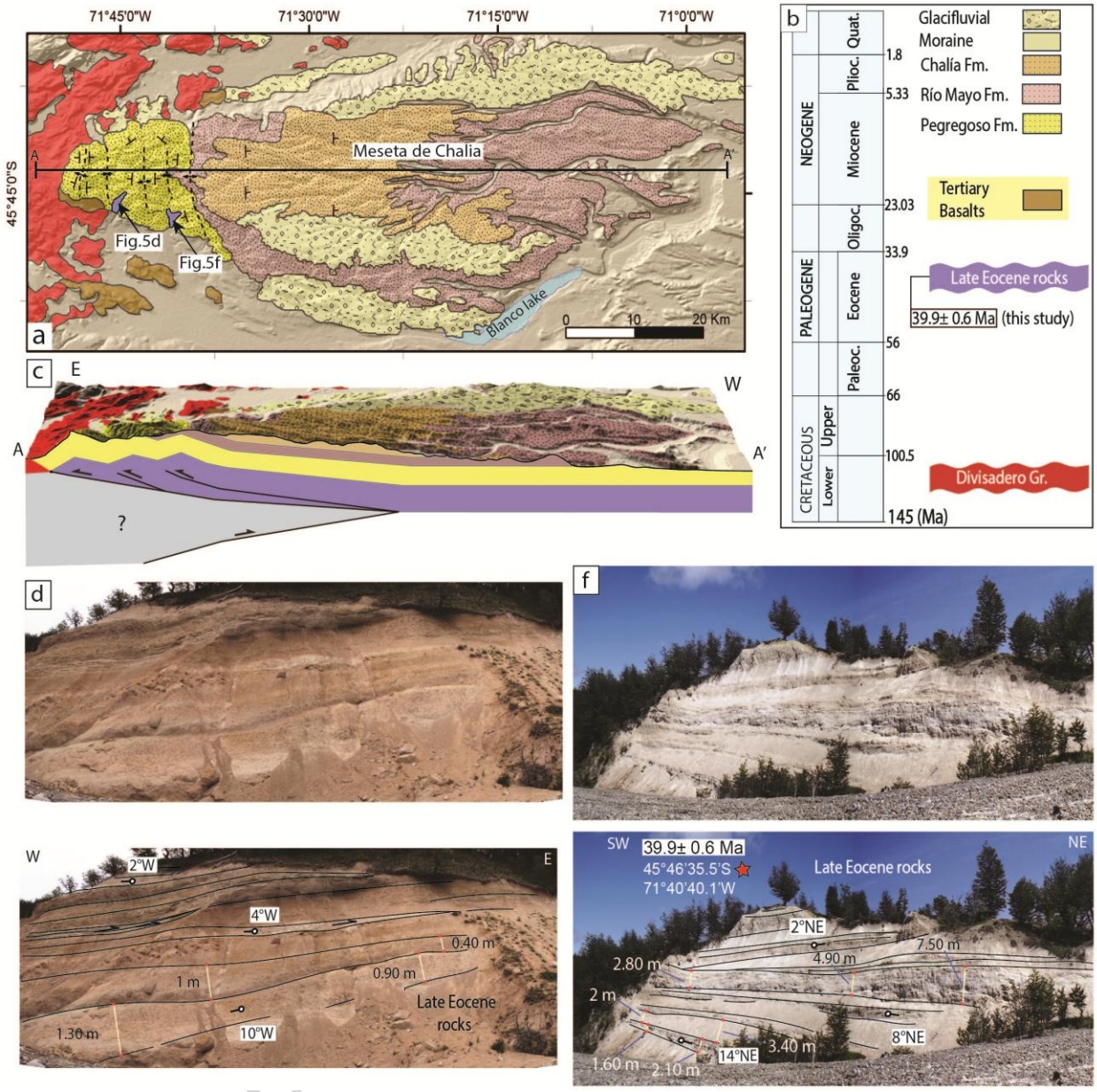

Fig. 5. (a) Sketch map and (b) stratigraphy of the Meseta de Chalía area (based on González, 1978; Dal Molin and Franchi, 1996 and this work). (c) Schematic structural cross-section of the Meseta de Chalía. (d and f) Eocene contractional growth-strata (see geochronology section 4.1) related to a west-vergent anticline.

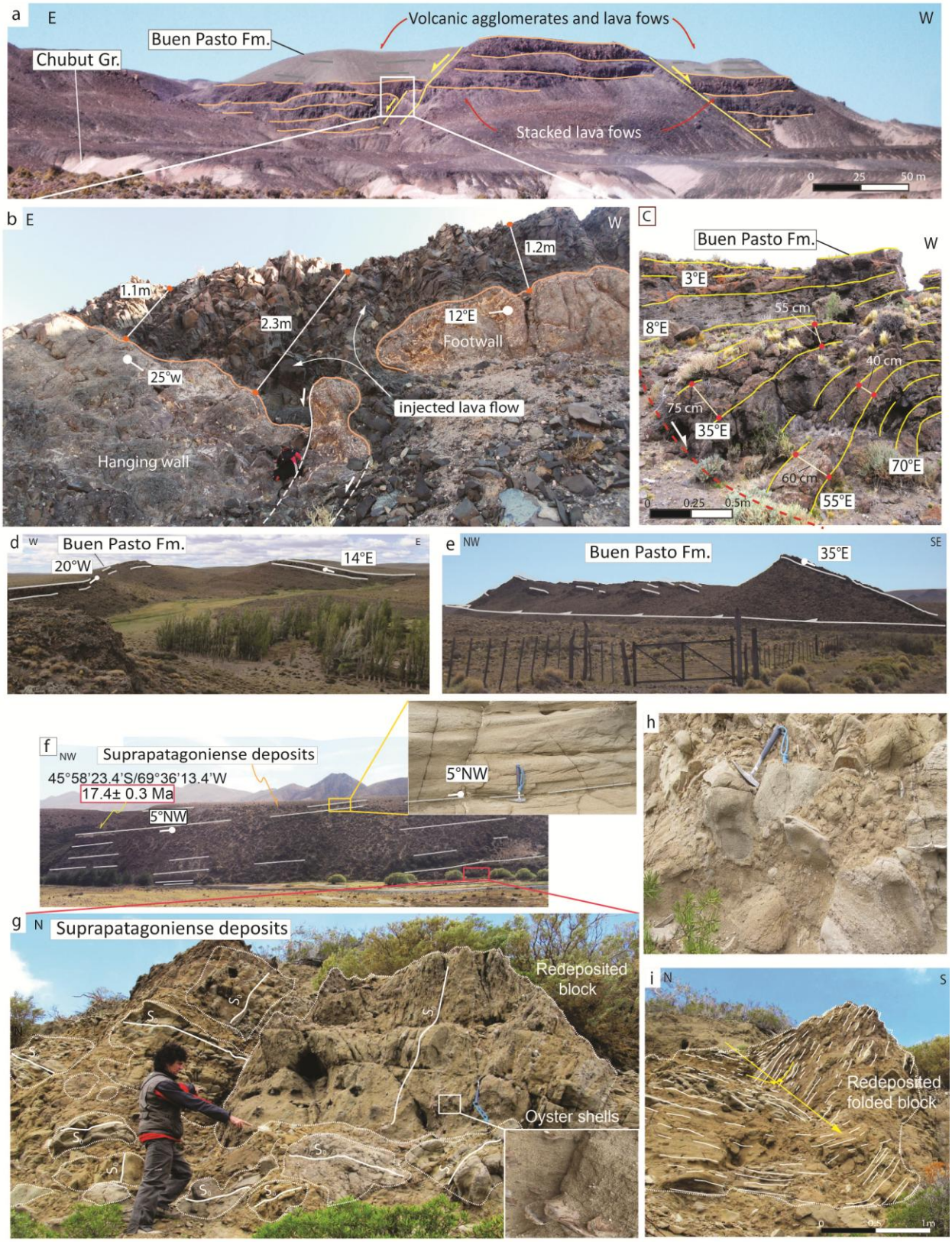

Fig. 6. (a) Extensional structures in late Oligocene/early Miocene Buen Pasto Formation. (b) Close-up to the eastern halfgraben showing volcanic injection controlled by normal faulting. (c) Synextensional growth-strata in volcanic agglomerates and lavas from the Buen Pasto Formation. (d) Typical open, asymmetric folds of the northwestern flank of the San Bernardo FTB. (e) West-vergent thrust in the Buen Pasto Formation, accounting for early-middle Miocene contraction (?). (f) Suprapatagoniense outcrops in the western limb of the Codo del Senguerr anticline, showing gently-dipping beds of sandstones dated in ~17 Ma. (g) Olistostrome deposits in Suprapatagoniense beds. S_0 indicates stratification plane. (h) Close-up to the sandy matrix with embedded smaller blocks. (i) Example of a tightly folded block inside the olistostrome. Yellow line indicates fold axial plane.

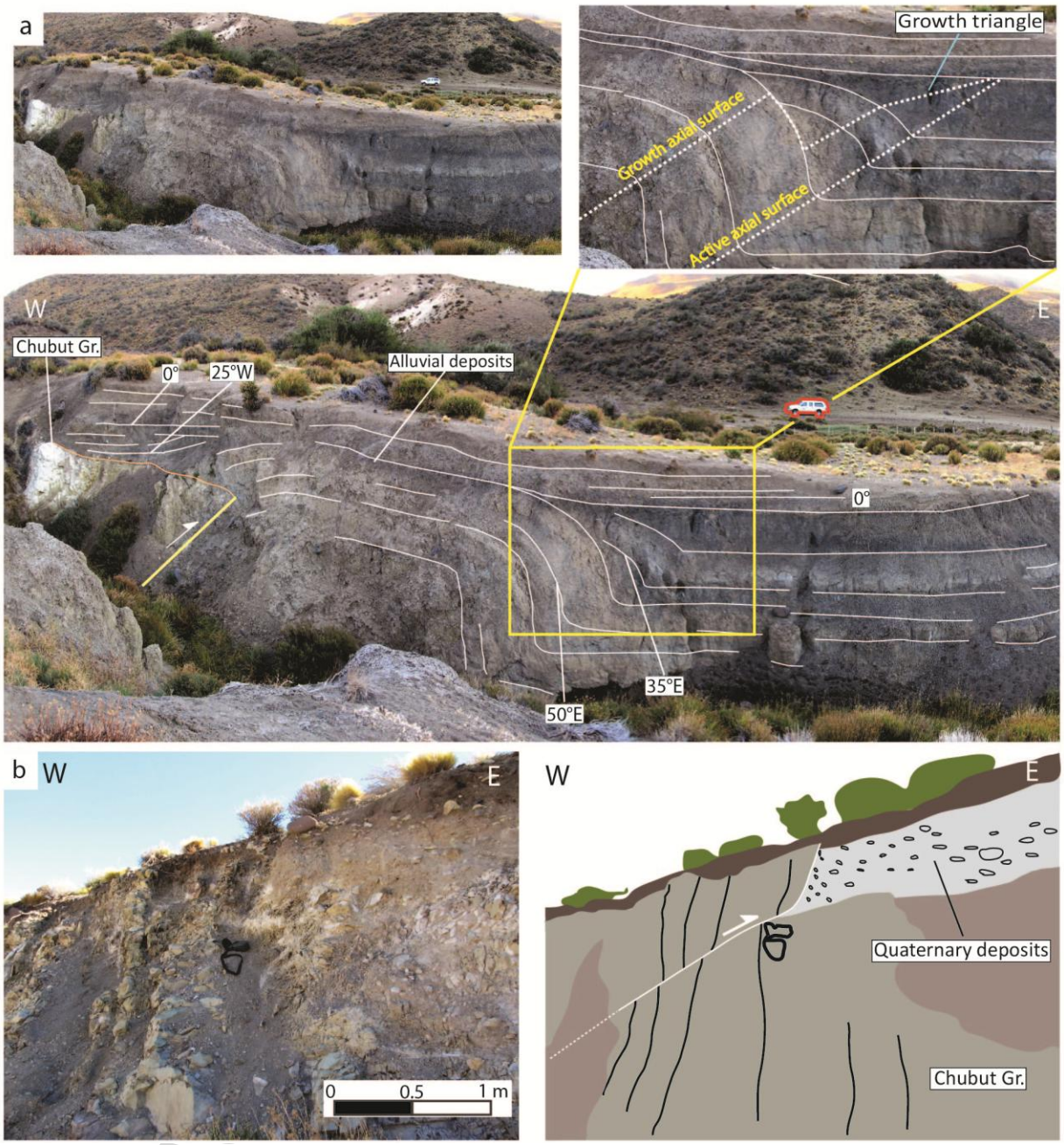

Fig. 7. Evidence of neotectonic activity in the San Bernardo FTB. See location in Fig. 2. (a) Reverse faulting and folding in Quaternary alluvial deposits. Inset image showing growth-strata geometry attesting for kink-band migration folding mechanisms. (b) Reverse fault that offsets Chubut Group strata overthrusting Quaternary deposits.

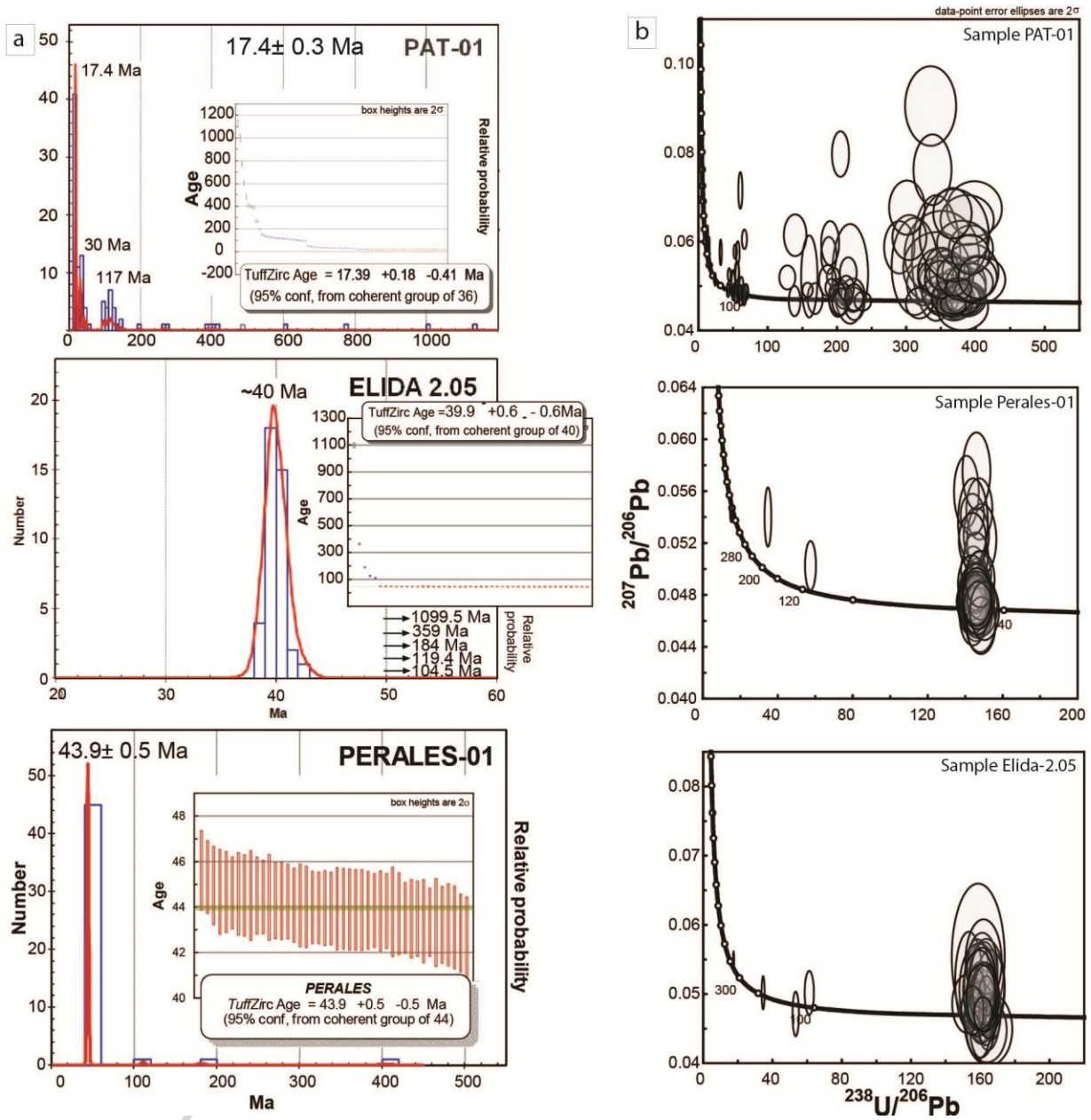

Fig. 8. Frequency histograms, relative probability plots of U-Pb detrital zircon ages (a) and Tera–Wasserburg concordia diagrams (b) of the PAT-02, Perales-01 and Elida-2.05 samples.

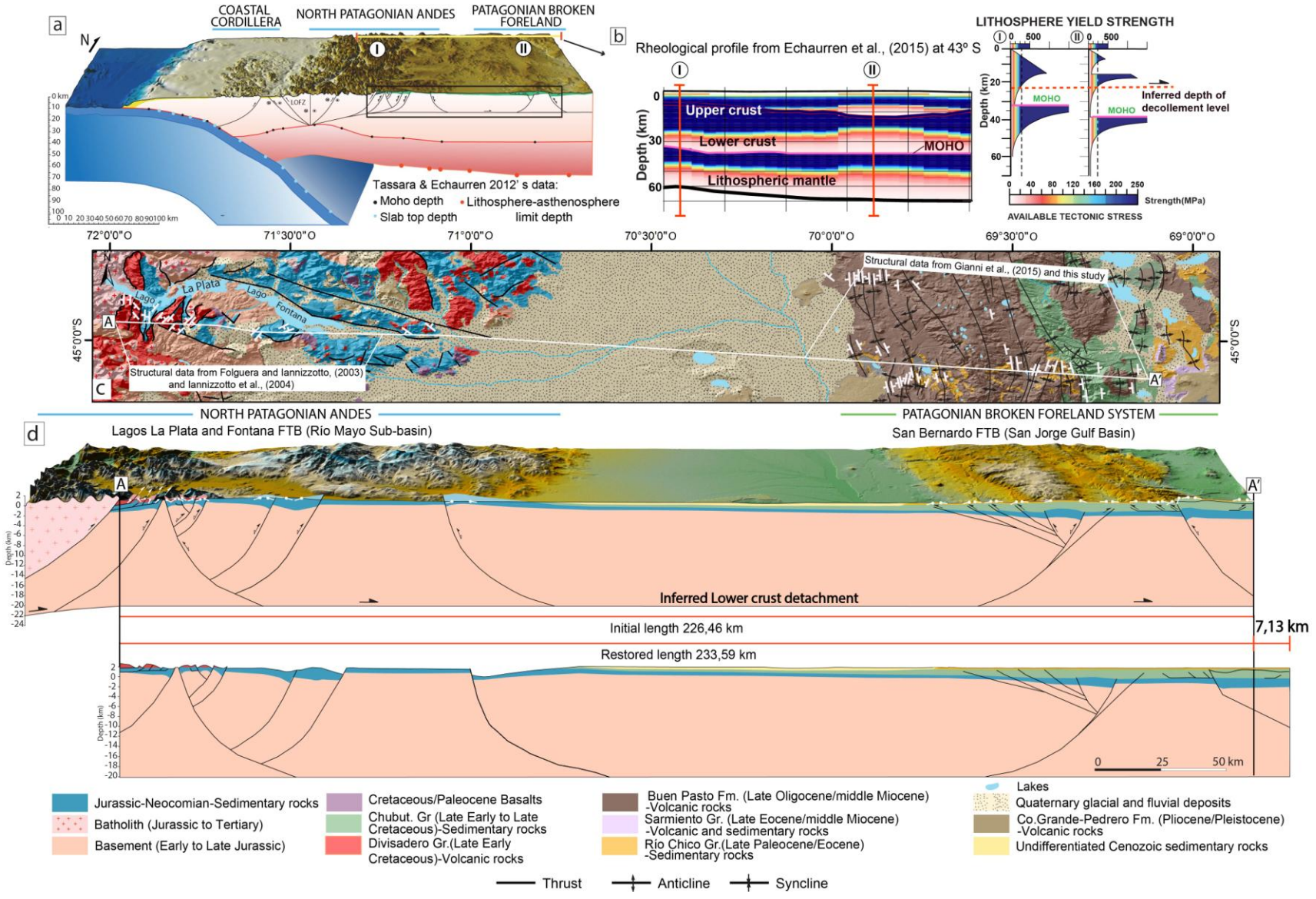

Fig. 9. (a) Lithospheric cross section at 45°S. Slab depth, Moho and lithosphere-asthenosphere Boundary (LAB) were obtained from Tassara and Echaurren (2012)'s gravity model. (b) Profile and strength envelopes from Echaurren et al. (2016) at 43ºS showing the rheological layering of the Patagonian foreland lithosphere showing inferred depth of detachment in the upper zone of the lower crust. (c) Location map of the cross section. See Fig. 1 for location. (d) Balanced and restored structural cross section from the Andes (Río Mayo Sub-basin) to the PBF (San Bernardo FTB) yielding a (minimum) total shortening of 7.13 km equivalent to a 3.14% of the initial length.

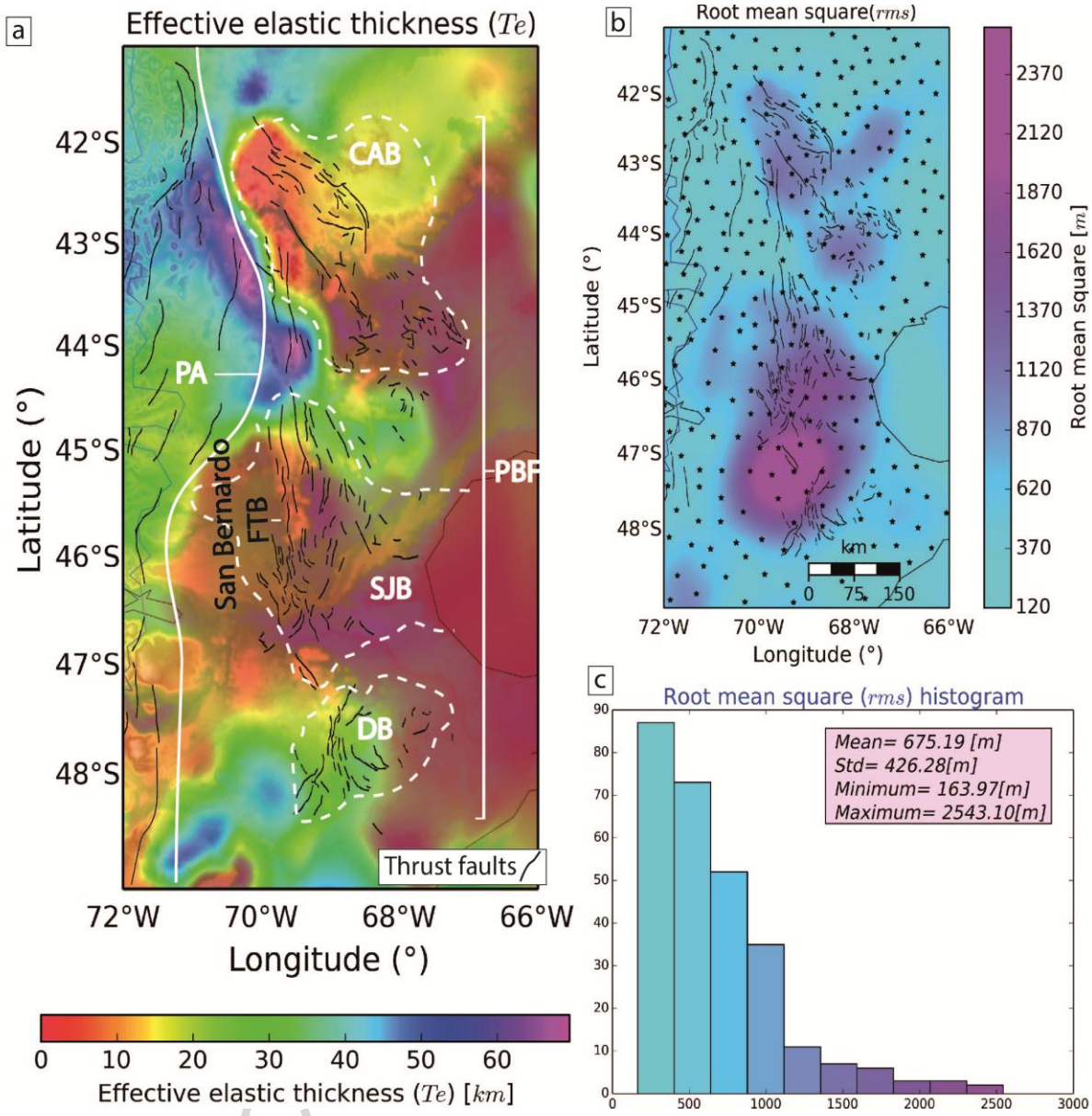

Fig. 10. (a) Effective elastic thickness map of Central Patagonia. Structures in (a) are from the compilation of Gianni et al. (2015a). Abbreviations are: PA: Patagonian Andes, CAB: Cañadón Asfalto Basin, SJGB: San Jorge Gulf Basin, DB: Deseado Basin. (b) Root mean square (rms) and grid of calculated areas. Black dots correspond to center points windows used in Te estimation (c) Histogram of rms.

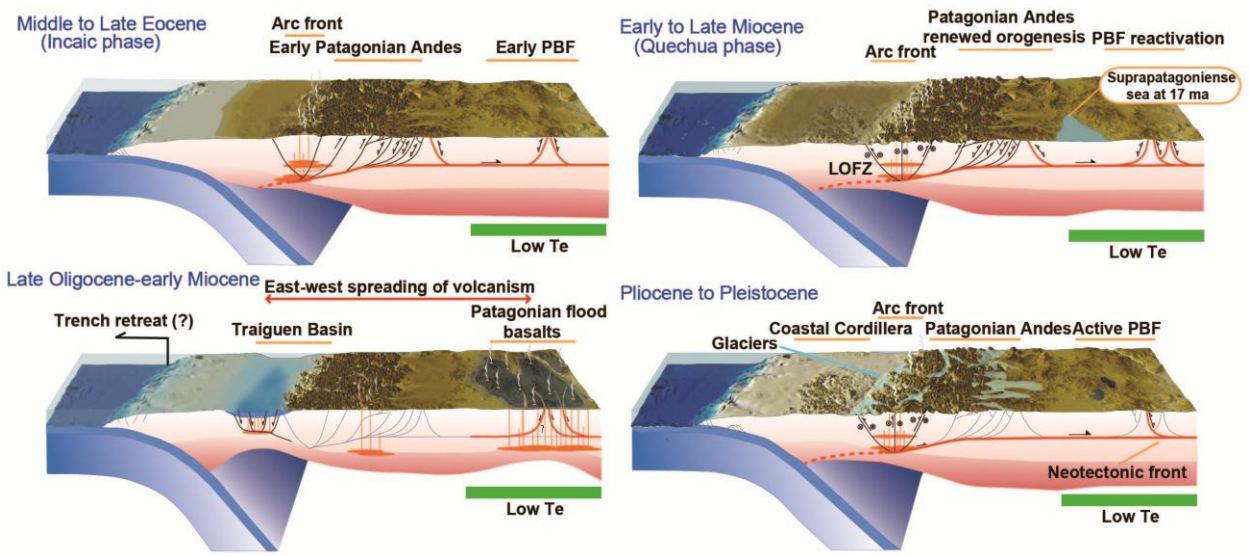

Fig. 11. Cenozoic evolution of the North Patagonian Andes and the central sector of PBF at 45ºS (see text for further details). LOFZ: Liquiñe-Ofqui fault zone.

TABLE

		P-wave velocity (V_p [Km/s])	**Density [g/cm^3]**	**Others parameters**
Topography			$\rho_t = 2.67$	
SJGB			$\rho_s = 2.32$	
Crust	**Upper crust**	6.35	$\rho_{us} = 2.69$	
	Lower crust		$\rho_{lc} = 2.89$	
Upper mantle		8.10	$\rho_m = 3.33$	
Poisson ratio				$\nu = 0.25$
Young modulus				$E = 10^{11}$ [Pa]
Gravity				$g = 9.8$ [m/s^2]
Normal crust thickness				$t = 35$ [km]

Table 1. Parameters used to estimate the effective elastic thickness in Central Patagonia. P-wave velocities were obtained from Chulick et al. (2013) and converted to density values through the equations of Brocher (2005). Topography (ρ_t) and sediment infill (ρ_s) densities were obtained from Hinze (2003) and Cornaglia et al. (2009), respectively.

Graphical abstract

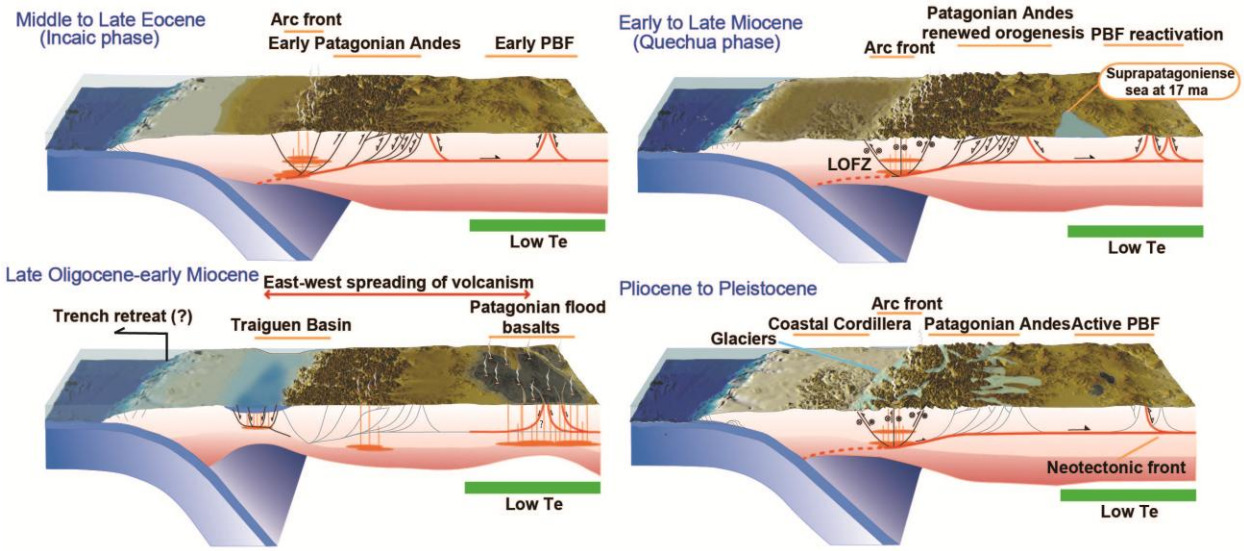

Highlights:

- Times and location of deformation in the Patagonian broken foreland remain enigmatic
- Description of syntectonic units unravels Cenozoic intraplate tectonics in Patagonia
- Deformation located in low elastic thickness areas far from the plate margin
- Previous intraplate extensional events could have weakened the foreland lithosphere